J|A|C|S
ARTICLES
Published on Web 05/09/2007

# Comparative Reactivity of TpRu(L)(NCMe)Ph (L = CO or $PMe_3$): Impact of Ancillary Ligand L on Activation of Carbon−Hydrogen Bonds Including Catalytic Hydroarylation and Hydrovinylation/Oligomerization of Ethylene

Nicholas A. Foley,[†] Marty Lail,[†] John P. Lee,[†] T. Brent Gunnoe,*[,†] Thomas R. Cundari,[‡] and Jeffrey L. Petersen[§]

*Contribution from the Department of Chemistry, North Carolina State University, Raleigh, North Carolina 27695-8204, Center for Advanced Scientific Computing and Modeling (CASCaM), Department of Chemistry, University of North Texas, Box 305070, Denton, Texas 76203-5070, and C. Eugene Bennett Department of Chemistry, West Virginia University, Morgantown, West Virginia 26506-6045*

Received November 28, 2006; E-mail: brent_gunnoe@ncsu.edu

***Abstract:*** Complexes of the type TpRu(L)(NCMe)R [L = CO or $PMe_3$; R = Ph or Me; Tp = hydridotris(pyrazolyl)borate] initiate C−H activation of benzene. Kinetic studies, isotopic labeling, and other experimental evidence suggest that the mechanism of benzene C−H activation involves reversible dissociation of acetonitrile, reversible benzene coordination, and rate-determining C−H activation of coordinated benzene. TpRu($PMe_3$)(NCMe)Ph initiates C−D activation of $C_6D_6$ at rates that are approximately 2−3 times more rapid than that for TpRu(CO)(NCMe)Ph (depending on substrate concentration); however, the catalytic hydrophenylation of ethylene using TpRu($PMe_3$)(NCMe)Ph is substantially less efficient than catalysis with TpRu(CO)(NCMe)Ph. For TpRu($PMe_3$)(NCMe)Ph, C−H activation of ethylene, to ultimately produce TpRu($PMe_3$)($\eta^3$-$C_4H_7$), is found to kinetically compete with catalytic ethylene hydrophenylation. In THF solutions containing ethylene, TpRu($PMe_3$)(NCMe)Ph and TpRu(CO)(NCMe)Ph separately convert to TpRu(L)($\eta^3$-$C_4H_7$) (L = $PMe_3$ or CO, respectively) via initial Ru-mediated ethylene C−H activation. Heating mesitylene solutions of TpRu(L)($\eta^3$-$C_4H_7$) under ethylene pressure results in the catalytic production of butenes (i.e., ethylene hydrovinylation) and hexenes.

## Introduction

Metal-mediated activation of carbon−hydrogen bonds is a key step in promising strategies for the functionalization of aliphatic and aromatic compounds.[1−9] Stoichiometric C−H activation reactions are now known for a diversity of transition metal systems, many of which operate at ambient conditions with high selectivity. Several mechanisms have been delineated for metal-mediated C−H activation including oxidative addition, $\sigma$-bond metathesis, electrophilic substitution, and 1,2-addition across metal−heteroatom bonds.[4,10] While much is understood about metal-mediated activation of C−H bonds, incorporation into catalytic cycles for C−H functionalization remains a substantial challenge.[2,5,11]

Catalytic Suzuki, Heck, Sonogashira, Stille, Negishi, and related reactions provide useful methods for C−C bond formation involving aromatic substrates.[12−18] However, such reactions require the incorporation of halide functionality into the aromatic substrate, which is often a low yield process that generates halogen-containing waste. Furthermore, with the exception of the Heck reaction, these catalytic cycles typically generate a stoichiometric quantity of metal-containing waste. In contrast, the direct addition of aromatic C−H bonds across olefin C=C bonds (i.e., olefin hydroarylation) provides an atom-economical

[†] North Carolina State University.
[‡] University of North Texas.
[§] West Virginia University.

(1) Davies, J. A.; Watson, P. L.; Liebman, J. F.; Greenberg, A. *Selective Hydrocarbon Activation*; VCH: New York, 1990.
(2) Ritleng, V.; Sirlin, C.; Pfeffer, M. *Chem. Rev.* **2002**, *102*, 1731−1769.
(3) Arndtsen, B. A.; Bergman, R. G.; Mobley, T. A.; Peterson, T. H. *Acc. Chem. Res.* **1995**, *28*, 154−162.
(4) Labinger, J. A.; Bercaw, J. E. *Nature* **2002**, *417*, 507−514.
(5) Goj, L. A.; Gunnoe, T. B. *Curr. Org. Chem.* **2005**, *9*, 671−685.
(6) Goldman, A. S.; Goldberg, K. I. *Organometallic C-H Bond Activation*; American Chemical Society: Washington, DC, 2004; Vol. 885, pp 1−43.
(7) Freund, M. S.; Labinger, J. A.; Lewis, N. S.; Bercaw, J. E. *J. Mol. Catal.* **1994**, *87* (1), L11−L15.
(8) Guari, Y.; Sabo-Etienne, S.; Chaudret, B. *Eur. J. Inorg. Chem.* **1999**, 1047−1055.
(9) Periana, R. A.; Bhalla, G.; Tenn, W. J.; Young, K. J. H.; Liu, X. Y.; Mironov, O.; Jones, C. J.; Ziatdinov, V. R. *J. Mol. Catal., A: Chem.* **2004**, *220* (1), 7−25.
(10) Lersch, M.; Tilset, M. *Chem. Rev.* **2005**, *105*, 2471−2526.
(11) Crabtree, R. H. *J. Chem. Soc., Dalton Trans.* **2001**, 2437−2450.
(12) Beletskaya, I. P.; Cheprakov, A. V. *Chem. Rev.* **2000**, *100*, 3009−3066.
(13) Hassan, J.; Sévignon, M.; Gozzi, C.; Schulz, E.; Lemaire, M. *Chem. Rev.* **2002**, *102*, 1359−1469.
(14) Fanta, P. E. *Synthesis* **1974**, 9−21.
(15) Bolm, C.; Hildebrand, J. P.; Muniz, K.; Hermanns, N. *Angew. Chem., Int. Ed.* **2001**, *40*, 3284−3308.
(16) Stille, J. K. *Angew. Chem., Int. Ed. Engl.* **1986**, *25*, 508−524.
(17) Miyaura, N.; Suzuki, A. *Chem. Rev.* **1995**, *95*, 2457−2483.
(18) Heck, R. F., Vinyl Substitutions with Organopalladium Intermediates. In *Complete Organic Syntheses*; Trost, B. M., Fleming, I., Semmelhack, M. F., Eds.; Pergamon Press: Oxford, U.K., 1999; Vol. 4, pp 833−863.

***Scheme 1.*** Depiction of Hydroarylation of Olefin Using Benzene and Ethylene as Substrates

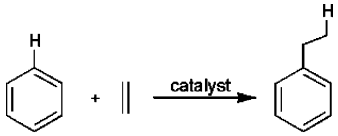


method for the formation of C−C bonds with aromatic substrates (Scheme 1).[19−40]

In addition to potential utility for synthetic organic chemistry, catalytic hydroarylation of olefins via pathways that involve metal-mediated C−H activation offers the possibility of efficient routes for the production of commodity scale chemicals such as ethylbenzene, cumene, and long-chain alkylbenzenes, which are manufactured on a multibillion pound scale annually.[41] The traditional means of production of these substrates involves Friedel−Crafts catalysis and suffers from drawbacks including low catalytic turnovers, use of acid cocatalysts, lack of control over linear/branched ratios, polyalkylation, and inability to recycle the catalyst.[42] Although advancements in solid-state catalysts have enhanced some aspects of alkyl arene production,[43] the methods remain less than ideal. Transition-metal-catalyzed hydroarylation of olefins via metal-mediated C−H activation offers possible alternative routes for C−C bond formation; however, examples of catalysis with nonactivated olefins are rare.[5,35−37,39,44−47]

***Scheme 2.*** Depiction of Metal-Catalyzed Olefin Hydroarylation (Shown in Red with Ethylene as Olefin Substrate) and Undesirable Side Reactions

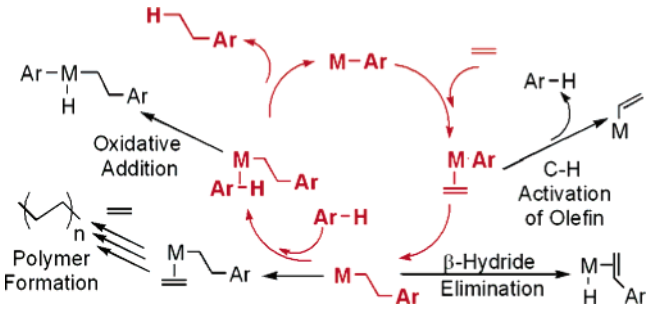


Our group has been investigating the use of $TpRu^{II}$ [Tp = hydridotris(pyrazolyl)borate] complexes as catalysts for the hydroarylation of olefins.[44−46,48−51] For example, TpRu(CO)(NCMe)Ph (**1**) catalytically produces ethylbenzene from ethylene and benzene and is, to our knowledge, the most active catalyst for the hydrophenylation of ethylene that proceeds through a metal-mediated C−H activation pathway.[44,45] Scheme 2 depicts a general catalytic cycle for olefin hydroarylation with common side reactions that can complicate catalysis. For example, irreversible $\beta$-hydride elimination, irreversible C−H oxidative addition, C−H activation of substrates other than the aromatic (e.g., olefin), and multiple insertions of olefin leading to oligomerization or polymerization of olefin can compete with the desired catalysis. Thus, an efficient catalyst must rapidly activate aromatic but not olefin C−H bonds. Furthermore, the catalyst must provide kinetic access to insertion of a single equivalent of olefin without catalyzing olefin oligomerization/polymerization. These demands result in a narrow window for successful catalyst development.

To develop improved catalysts for olefin hydroarylation rationally, it is necessary to understand the impact of catalyst features on various steps along and outside the catalytic cycle. Herein, we report on experimental and computational studies comparing the reactivity of TpRu(CO)(NCMe)Ph (**1**), our previously reported olefin hydroarylation catalyst, and TpRu(PMe$_3$)(NCMe)Ph (**2**), which bears the more strongly electron-donating and more sterically bulky PMe$_3$ ligand. Included are comparisons of (a) the relative rates of stoichiometric benzene C−H(D) activation, (b) the relative rates and pathways for ethylene C−H activation, (c) the efficacy for catalytic hydroarylation of olefins, and (d) catalytic hydrovinylation/oligomerization of ethylene. The results provide guidelines for the design of future catalysts.

## Results

**Stoichiometric Benzene C−H(D) Activation by TpRu(PMe$_3$)(NCMe)R (R = Me or Ph).** We have previously reported that TpRu(CO)(NCMe)R (R = Me or Ph) systems initiate stoichiometric C−H activation of aromatic substrates including benzene, furan, and thiophene, and mechanistic studies

(19) Murai, S.; Kakiuchi, F.; Sekine, S.; Tanaka, Y.; Kamatani, A.; Sonoda, M.; Chatani, N. *Nature* **1993**, *366*, 529−531.
(20) Murai, S.; Kakiuchi, F.; Sekine, S.; Tanaka, Y.; Kamatani, A.; Sonoda, M.; Chatani, N. *Pure App. Chem.* **1994**, *66*, 1527−1534.
(21) Thalji, R. K.; Ahrendt, K. A.; Bergman, R. G.; Ellman, J. A. *J. Am. Chem. Soc.* **2001**, *123*, 9692−9693.
(22) Tan, K. L.; Bergman, R. G.; Ellman, J. A. *J. Am. Chem. Soc.* **2001**, *123*, 2685−2686.
(23) Lenges, C. P.; Brookhart, M. *J. Am. Chem. Soc.* **1999**, *121*, 6616−6623.
(24) Weissman, H.; Song, X.; Milstein, D. *J. Am. Chem. Soc.* **2001**, *123*, 337−338.
(25) Jia, C.; Lu, W.; Kitamura, T.; Fujiwara, Y. *Org. Lett.* **1999**, *1*, 2097−2100.
(26) Karshtedt, D.; McBee, J. L.; Bell, A. T.; Tilley, T. D. *Organometallics* **2006**, *25* (7) 1801−1811.
(27) Jia, C.; Piao, D.; Oyamada, J.; Lu, W.; Kitamura, T.; Fujiwara, Y. *Science* **2000**, *287*, 1992−1995.
(28) Boele, M. D. K.; van Strijdonck, G. P. F.; de Vries, A. H. M.; Kamer, P. C. J.; de Vries, J. G.; van Leeuwen, P. W. N. M. *J. Am. Chem. Soc.* **2002**, *124*, 1586−1587.
(29) Pastine, S. J.; Youn, S. W.; Sames, D. *Org. Lett.* **2003**, *5*, 1055−1058.
(30) Youn, S. W.; Pastine, S. J.; Sames, D. *Org. Lett.* **2004**, *6*, 581−584.
(31) Shi, Z.; He, C. *J. Org. Chem.* **2004**, *69*, 3669−3671.
(32) Tan, K. L.; Park, S.; Ellman, J. A.; Bergman, R. G. *J. Org. Chem.* **2004**, *69* (21), 7329−7335.
(33) Han, X.; Widenhoefer, R. A. *Org. Lett.* **2006**, *8* (17), 3801−3804.
(34) Zhang, Z.; Wang, X.; Widenhoefer, R. A. *Chem. Commun.* **2006**, (35), 3717−3719.
(35) Matsumoto, T.; Taube, D. J.; Periana, R. A.; Taube, H.; Yoshida, H. *J. Am. Chem. Soc.* **2000**, *122*, 7414−7415.
(36) Matsumoto, T.; Periana, R. A.; Taube, D. J.; Yoshida, H. *J. Mol. Catal., A.: Chem.* **2002**, *180*, 1−18.
(37) Periana, R. A.; Liu, X. Y.; Bhalla, G. *Chem. Commun.* **2002**, *24*, 3000−3001.
(38) Oxgaard, J.; Muller, R. P.; Goddard, W. A., III; Periana, R. A. *J. Am. Chem. Soc.* **2004**, *126*, 352−363.
(39) Oxgaard, J.; Periana, R. A.; Goddard, W. A., III. *J. Am. Chem. Soc.* **2004**, *126*, 11658−11665.
(40) Bhalla, G.; Oxgaard, J.; Goddard, W. A., III; Periana, R. A. *Organometallics* **2005**, *24*, 3229−3232.
(41) Chenier, P. J. *Survey of Industrial Chemistry*, 2nd ed.; Wiley-VCH: New York, 1992.
(42) Olah, G. A.; Molnár, Á. *Hydrocarbon Chemistry*, 2nd ed.; Wiley-Interscience: New York, 2003; pp 229−232.
(43) Olah, G. A.; Molnár, Á. *Hydrocarbon Chemistry*, 2nd ed.; Wiley-Interscience: New York, 2003; pp 262−267.
(44) Lail, M.; Arrowood, B. N.; Gunnoe, T. B. *J. Am. Chem. Soc.* **2003**, *125*, 7506−7507.
(45) Lail, M.; Bell, C. M.; Conner, D.; Cundari, T. R.; Gunnoe, T. B.; Petersen, J. L. *Organometallics* **2004**, *23*, 5007−5020.
(46) Pittard, K. A.; Lee, J. P.; Cundari, T. R.; Gunnoe, T. B.; Petersen, J. L. *Organometallics* **2004**, *23*, 5514−5523.
(47) Bhalla, G.; Liu, X. Y.; Oxgaard, J.; Goddard, W. A., III; Periana, R. A. *J. Am. Chem. Soc.* **2005**, *127*, 11372−11389.
(48) Arrowood, B. N.; Lail, M.; Gunnoe, T. B.; Boyle, P. D. *Organometallics* **2003**, *22*, 4692−4698.
(49) Lail, M.; Gunnoe, T. B.; Barakat, K. A.; Cundari, T. R. *Organometallics* **2005**, *24*, 1301−1305.
(50) Pittard, K. A.; Cundari, T. R.; Gunnoe, T. B.; Day, C. S.; Petersen, J. L. *Organometallics* **2005**, *24*, 5015−5024.
(51) Goj, L. A.; Lail, M.; Pittard, K. A.; Riley, K. C.; Gunnoe, T. B.; Petersen, J. L. *Chem. Commun.* **2006**, (9), 982−984.

***Scheme 3.*** Proposed Pathway for Benzene C−H Activation by TpRu(L)(NCMe)R {L = CO or $PMe_3$; R = Me or Ph; [Ru] = Concentration of Starting Ru Complex TpRu(CO)(NCMe)R or TpRu($PMe_3$)(NCMe)R}

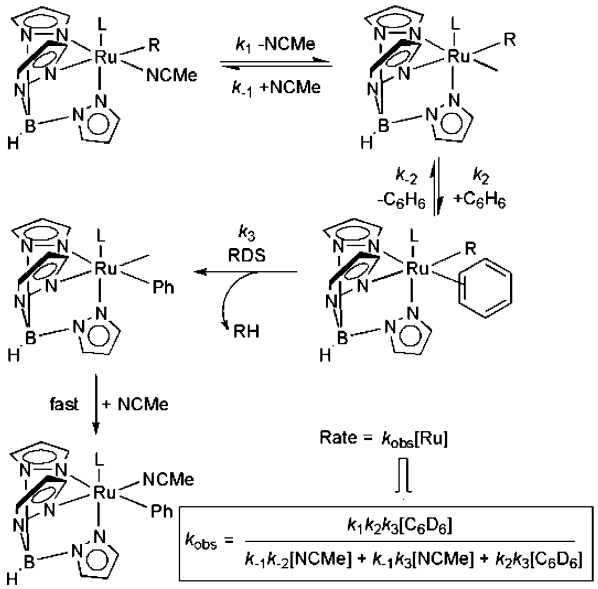


of the C−H activation process are consistent with the pathway depicted in Scheme 3.[44,46] Reversible dissociation of acetonitrile provides a site for benzene (or other aromatic) coordination, and subsequent coordination of benzene (reversible) and C−H activation produces R−H and TpRu(CO)(NCMe)Ph (**1**). Density functional theory (DFT) calculations indicate a transition state for the C−H activation step that resembles $\sigma$-bond metathesis.[45] Jia and Eisenstein et al. have reported similar results for calculations of closely related TpRu systems,[52] while Lau et al. have reported calculations for C−H activation by TpRu($PPh_3$)H that suggest the transition states reflect oxidative addition of the C−H bond.[53] A close Ru−H contact in the calculated C−H activation transition state for TpRu(CO)R, as well as a similar interaction for an isoelectronic Ir system, has prompted Goddard et al. to label the transition state as an "oxidative hydrogen migration."[39,45,54]

For both the stoichiometric C−H activation of benzene and the hydrophenylation of ethylene catalyzed by **1**, the rate-determining step (RDS) is likely the benzene C−H activation event. This assertion is based on the observation of primary intermolecular kinetic isotope effects with $k_H/k_D = 2.1(1)$ for catalytic hydroarylation reaction and $k_H/k_D = 2.5(5)$ for stoichiometric benzene activation by TpRu(CO)(NCMe)Me.[45] Thus, to increase the rate of catalytic olefin hydroarylation, it is necessary to decrease the activation barrier of metal-mediated aromatic C−H activation. Although this rationale may be overly simplistic,[55] the predicted oxidative character of the calculated transition state (i.e., calculated Ru−H contact; see above) suggests the possibility that increasing metal-based electron density might reduce the barrier to the aromatic C−H activation step. To begin to formulate an understanding of the impact of ancillary ligands on the energetics of benzene C−H activation, we have compared the rates of $C_6D_6$ activation by TpRu(L)(NCMe)R (R = Me or Ph; L = CO or $PMe_3$). The rate law for the proposed mechanism is depicted in Scheme 3.

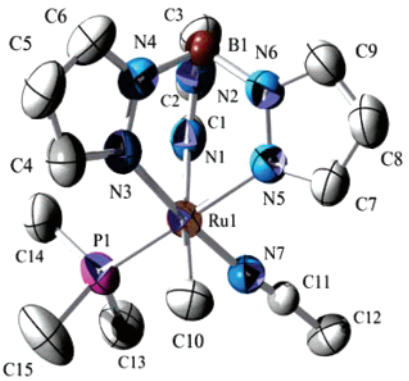


***Figure 1.*** ORTEP of TpRu($PMe_3$)(NCMe)Me (**3**) (30% probability with hydrogen atoms omitted). Selected bond lengths (Å): Ru1−N7, 1.989(2); Ru1−C10, 2.129(3); Ru1−P1, 2.253(1); Ru1−N1, 2.170(2); Ru1−N3, 2.080(2); Ru1−N5, 2.135(2); N7−C11, 1.145(3); C11−C12, 1.438(4); Selected bond angles (deg): N7−Ru1−C10, 88.6(1); N7−Ru1−P1, 92.0(1); C10−Ru1−P1, 91.0(1); N7−C11−C12, 179.2(3).

***Table 1.*** Selected Crystallographic Data for TpRu($PMe_3$)(NCMe)Me (**3**) and TpRu($PMe_3$)(CN$^t$Bu)Ph (**4**)

| param | complex **3** | complex **4** |
|---|---|---|
| empirical formula | $C_{15}H_{25}BN_7PRu$ | $C_{23}H_{33}BN_7PRu$ |
| fw | 446.27 | 550.41 |
| cryst system | orthorhombic | monoclinic |
| space group | *Pbca* | $P2_1$ |
| *a*, Å | 14.0332(9) | 9.8198(9) |
| *b*, Å | 15.911(1) | 13.232(1) |
| *c*, Å | 18.882(1) | 11.018(1) |
| $\beta$, deg | | 116.414(1) |
| *V*, Å$^3$ | 4216.0(5) | 1282.2(2) |
| *Z* | 8 | 2 |
| $D_{calcd}$, g/cm$^3$ | 1.406 | 1.426 |
| cryst size, mm | 0.30 × 0.36 × 0.38 | 0.05 × 0.20 × 0.38 |
| R1, wR2 [$I > 2(I)$] | 0.0337, 0.0815 | 0.0449, 0.1097 |
| GOF | 1.041 | 1.028 |

TpRu($PMe_3$)(NCMe)Me (**3**) is prepared upon reaction of TpRu($PMe_3$)(NCMe)OTf (OTf = trifluoromethanesulfonate) with $Me_2Mg$ and is isolated in 60% yield. In addition to multinuclear NMR spectroscopy and elemental analysis, complex **3** has been characterized by a solid-state X-ray diffraction study (Figure 1; Table 1). The structure of **3** reveals a pseudooctahedral coordination sphere with little deviation from the octahedral paradigm. The Ru−Me bond distance of 2.129(3) Å is comparable to previously reported Ru−Me bond lengths including Tp*Ru($\eta^4$-cyclooctadiene)Me [Tp* = hydridotris(3,5-dimethylpyrazolyl)borate], 2.159(4) Å,[56] $(S)_{Ru}$-Ru(neomenthylcyclopentadienyl)(CO)($PPh_3$)Me, 2.165(16) Å,[57] [($\eta^6$-$C_6H_6$)Ru(Me)($PPh_3$)$_2$][$AlMe_2Cl_2$], 2.124(9) Å,[58] and [Ru(bpy)$_2$(CO)Me][$PF_6$] (bpy = 2,2-bipyridine), 2.21(2) Å.[59]

Heating **3** in $C_6D_6$ in a sealed NMR tube produces **2**-$d_5$ in quantitative yield and $CH_3D$ (1:1:1 triplet at ~0.15 ppm in $^1$H

(52) Lam, W. H.; Jia, G.; Lin, Z.; Lau, C. P.; Eisenstein, O. *Chem.—Eur. J.* **2003**, *9*, 2775−2782.
(53) Ng, S. M.; Lam, W. H.; Mak, C. C.; Tsang, C. W.; Jia, G. C.; Lin, Z. Y.; Lau, C. P. *Organometallics* **2003**, *22* (4), 641−651.
(54) Oxgaard, J.; Goddard, W. A., III. *J. Am. Chem. Soc.* **2004**, *126*, 442−443.
(55) Krogh-Jespersen, K.; Czerw, M.; Zhu, K.; Singh, B.; Kanzelberger, M.; Darji, N.; Achord, P. D.; Renkema, K. B.; Goldman, A. S. *J. Am. Chem. Soc.* **2002**, *124*, 10797−10809.
(56) Corrochano, A. E.; Jalón, F. A.; Otero, A.; Kubicki, M. M.; Richard, P. *Organometallics* **1997**, *16*, 145−148.
(57) Lindsay, C.; Cesarotti, E.; Adams, H.; Bailey, N. A.; White, C. *Organometallics* **1990**, *9*, 2594−2602.
(58) Fang, K.; Watkin, J. G.; Scott, B. L.; John, K. D.; Kubas, G. J. *Organometallics* **2002**, *21*, 2336−2339.
(59) Ooyama, D.; Tomon, T.; Tsuge, K.; Tanaka, K. *J. Organomet. Chem.* **2001**, *619*, 299−304.

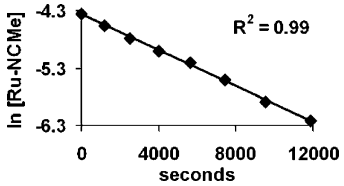


***Figure 2.*** Sample first-order plot for acetonitrile exchange of TpRu($PMe_3$)(NCMe)Ph (**2**) in $NCCD_3$ at 60 °C. The *y*-axis [ln(Ru−NCMe)] is taken from the disappearance of coordinated protio-NCMe by $^1H$ NMR spectroscopy.

NMR spectrum) after approximately 24 h at 70 °C (eq 1). Heating **3** in a 1:1 molar ratio of $C_6D_6$ and $C_6H_6$ produces $CH_3D$ and $CH_4$. Analysis of resonances due to methane and methane-$d_1$ of multiple reactions using $^1H$ NMR spectroscopy reveals an average $k_H/k_D = 2.7(1)$. Thus, similar to stoichiometric benzene activation by TpRu(CO)(NCMe)Me, *the intermolecular primary kinetic isotope effect for **3** is consistent with C−H(D) activation of coordinated benzene as the RDS*. Furthermore, the similar primary kinetic isotope effects (KIEs) measured for TpRu(CO)(NCMe)Me [$k_H/k_D = 2.5(5)$] and complex **3** suggest that benzene C−H(D) activation by TpRu(L)($\eta^2$-benzene)R (L = CO or $PMe_3$) may have geometrically similar transition states, a conjecture supported by DFT calculations (see below).

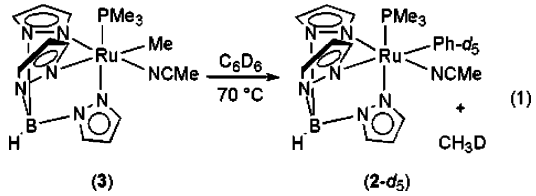


Because benzene C−H activation is suggested to involve acetonitrile dissociation by TpRu(L)(NCMe)R systems, the lability of the acetonitrile ligand of **2** was gauged through degenerate ligand exchange with $NCCD_3$ at 60 °C by monitoring the disappearance of the resonance due to the acetonitrile ligand through 3 half-lives. Determination of $k_{obs}$ for the NCMe/$NCCD_3$ exchange from three separate experiments yielded an average pseudo-first-order $k_{obs}$ of $1.5(1) \times 10^{-4}$ $s^{-1}$ (Figure 2), which is more rapid than the rate of benzene activation (see below). The rate of ligand exchange at 60 °C between coordinated NCMe and free $NCCD_3$ is approximately 5 times more rapid for the $PMe_3$ complex **2** than for TpRu(CO)(NCMe)Ph (**1**) [$k_{obs} = 3.2(2) \times 10^{-5}$ $s^{-1}$] at 70 °C.

In $C_6D_6$ at 70 °C, complex **2** reacts to produce $C_6H_5D$ and **2**-$d_5$ (eq 2). After 72 h, $^1H$ NMR spectroscopy reveals the absence of resonances due to the phenyl ligand, and $^2H$ NMR spectroscopy shows the emergence of two broad peaks at 7.25 and 7.10 ppm, nearly coincident with the reported chemical shifts of the protio-phenyl ligand of complex **2**.[60] In addition, as previously reported, regioselective H/D exchange at the Tp-4 positions of the tris(pyrazolyl)borate ligand is observed.[60]

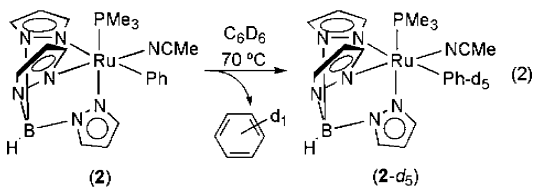


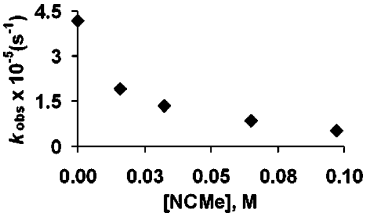


***Figure 3.*** Plot of the $k_{obs}$ for $C_6D_6$ activation by TpRu($PMe_3$)(NCMe)Ph (**2**) versus concentration of free acetonitrile at 60 °C in $C_6D_6$. Each data point ($k_{obs}$) is an average of at least three experiments.

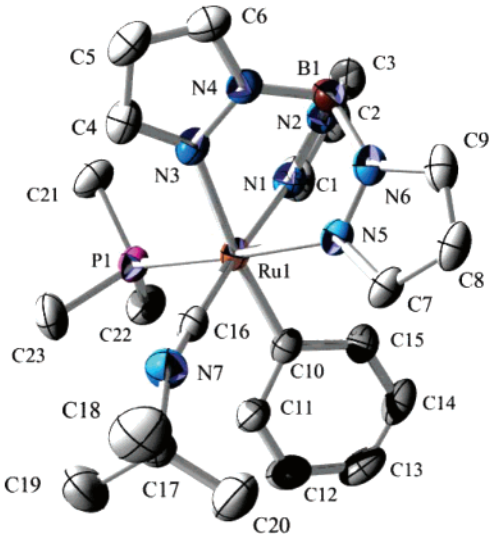


***Figure 4.*** ORTEP of TpRu($PMe_3$)($CN^tBu$)Ph (**4**) (30% probability with hydrogen atoms omitted). Selected bond lengths (Å): Ru1−C16, 1.882(5); Ru1−P1, 2.280(1); Ru1−C10, 2.065(4); N7−C16, 1.160(6); N7−C17, 1.451(7); C10−C11, 1.401(6). Selected bond angles (deg): Ru1−C16−N7, 177.3(4); C16−N7−C17, 157.5(5); C16−Ru1−C10, 87.3(2); C10−Ru1−P1, 92.8(1); C16−Ru1−P1, 92.1(1); C16−Ru1−N1, 175.3(2).

The rate of $C_6D_6$ activation by **2** as a function of free acetonitrile concentration was determined. Figure 3 shows a plot of $k_{obs}$ versus concentration of free acetonitrile. Each $k_{obs}$ in the plot (Figure 3) is an average of at least three independent experiments. The inverse dependence of $k_{obs}$ on concentration of NCMe is consistent with the proposed mechanism and the corresponding rate law (Scheme 3).

As additional verification that acetonitrile dissociation is involved in benzene activation, TpRu($PMe_3$)($CN^tBu$)Ph (**4**) was independently synthesized by heating **2** in benzene with 3 equiv of *tert*-butyl isonitrile ($CN^tBu$) for 2 h. Complex **4** has been characterized by multinuclear NMR spectroscopy, elemental analysis, and a solid-state X-ray diffraction study of a single crystal (Figure 4; Table 1), the latter revealing a pseudooctahedral coordination sphere. The observed $\nu_{CN}$ for **4** of 2031 $cm^{-1}$ compared with the absorption for free isonitrile (2136 $cm^{-1}$) reveals Ru-to-isonitrile d$\pi$ backbonding.

It is anticipated that the isonitrile ligand of **4** is more strongly coordinated than the acetonitrile ligand of **2**. Consistent with this notion and the proposed involvement of the five-coordinate system {TpRu($PMe_3$)Ph} in the benzene C−H(D) activations,

(60) Feng, Y.; Lail, M.; Foley, N. A.; Gunnoe, T. B.; Barakat, K. A.; Cundari, T. R.; Petersen, J. L. *J. Am. Chem. Soc.* **2006**, *128*, 7982−7994.

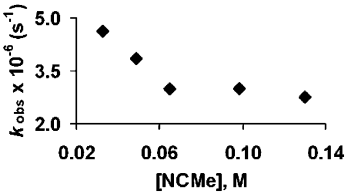


***Figure 5.*** Plot of $k_{obs}$ for $C_6D_6$ activation by TpRu(CO)(NCMe)Ph (**1**) versus concentration of free NCMe at 60 °C. Each data point ($k_{obs}$) is an average of at least three experiments.

heating complex **4** in $C_6D_6$ for 3 days at 60 °C results in no observable change by $^1$H NMR spectroscopy (eq 3).

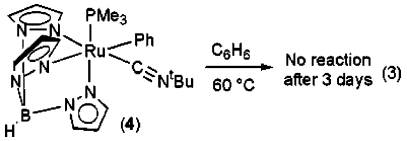


**Comparative Study of Benzene C−H Activation.** To directly compare the impact of ancillary ligand "L" on the overall rate of benzene C−H activation by TpRu(L)(NCMe)Ph (L = CO or $PMe_3$), we studied the reaction of **1** and $C_6D_6$. In addition to the formation of TpRu(CO)(NCMe)Ph-$d_5$ (**1**-$d_5$) and $C_6H_5D$, the reaction of complex **1** and $C_6D_6$ at elevated temperatures in the absence of added NCMe results in partial decomposition of **1** to uncharacterized products. However, the addition of free NCMe suppresses the decomposition and allows reproducible kinetics for the nearly quantitative conversion of **1** and $C_6D_6$ to **1**-$d_5$ and $C_6H_5D$. The rate of this reaction was determined by independent reactions with 1, 1.5, 2, 3, and 4 equiv of free NCMe with respect to complex **1** (Figure 5). Each $k_{obs}$ in the plot (Figure 5) is an average of at least three independent experiments. As with complex **2**, the plot is consistent with the rate law in Scheme 3.

Table 2 displays the ratio of $k_{obs}$ for $C_6D_6$ activation by complexes **1** and **2** with variable concentration of free acetonitrile. The *overall* rate of benzene C−D activation by TpRu(L)(NCMe)Ph is approximately 2−3 times more rapid for L = $PMe_3$ than for L = CO over the range of NCMe concentrations. The difference in rate of benzene C−H activation represents a relatively small overall difference in $\Delta G^{\ddagger}$ ($\Delta G^{\ddagger}$'s for the reactions cannot be calculated since rate constants, $k_{obs}$, are a combination of multiple step rate constants and terms for the concentration of benzene and NCMe).

**Catalytic Hydrophenylation of Ethylene.** We have previously reported that complex **1** catalyzes the hydroarylation of olefins as depicted in Scheme 4.[44,45] Using the mechanism in Scheme 4, the overall catalyst activity is determined by the rates of olefin coordination, olefin insertion into the Ru−aryl bond, aromatic coordination, and aromatic C−H activation. The latter step has been shown to be the likely RDS in both catalytic and stoichiometric benzene C−H activation by TpRu(L)(NCMe)R systems.[45] Above, we disclosed data consistent with an increase in the overall rate of benzene C−H activation upon substitution of the CO ligand with $PMe_3$. Given that aromatic C−H activation is the proposed RDS in the catalytic hydrophenylation of ethylene, this suggests that TpRu($PMe_3$)(NCMe)Ph (**2**) *might be* a more active catalyst than TpRu(CO)(NCMe)Ph (**1**) for the hydroarylation of olefins.

***Scheme 4.*** Catalytic Hydroarylation of Olefins (Benzene and Ethylene Shown) Using TpRu(L)(NCMe)Ph (L = CO or $PMe_3$)

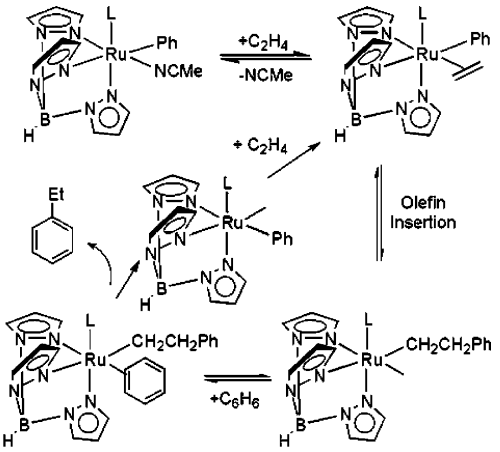


Using complex **2** as catalyst (0.1 mol %), we explored the catalytic hydrophenylation of ethylene in benzene. Analysis of various reaction conditions ranging from 25 to 900 psi of ethylene and 60 to 180 °C, maximum production of ethylbenzene was achieved at 800 psi of ethylene at 180 °C (Table 3). Under these conditions, 3.6 equiv of ethylbenzene and 2.5 equiv of styrene (based on **2**) are observed after 12 h. For most reaction conditions, analysis of the catalyst mixture after heating revealed the near-quantitative production (by $^1$H NMR spectroscopy) of the $\eta^3$-allyl complex TpRu($PMe_3$)($\eta^3$-$C_4H_7$) (**5**) (see below for characterization details of complex **5**). Attempted catalysis with 1-hexene produced no alkylbenzene under variable conditions. Thus, the $PMe_3$ complex **2** is clearly a less efficient catalyst for the hydroarylation of olefins than is the CO complex **1**.

**Reaction of TpRu(L)(NCMe)Ph with Ethylene.** Having observed the formation of the $\eta^3$-allyl complex TpRu($PMe_3$)($\eta^3$-$C_4H_7$) (**5**) during attempted hydrophenylation of ethylene, we sought more details for the formation of **5**. The reaction of **2** with ethylene (250 psi) in THF at 70 °C produces **5** in ∼90% isolated yield (eq 4). Analyses of crude reaction mixtures by $^1$H NMR spectroscopy suggest that **5** is formed quantitatively from **2** and ethylene under these conditions (note: lower

***Table 2.*** Comparison of $k_{obs}$ (60 °C; kcal/mol) for $C_6D_6$ Activation by TpRu(CO)(NCMe)Ph (**1**) and TpRu($PMe_3$)(NCMe)Ph (**2**)

| [NCMe][a] | $k_{obs}$(**2**)/$k_{obs}$(**1**) |
|---|---|
| 0.03 | 2.9 |
| 0.07 | 2.8 |
| 0.10 | 1.8 |

[a] M.

***Table 3.*** Hydrophenylation of Ethylene by TpRu($PMe_3$)(NCMe)Ph (**2**) (0.1 mol %) in Benzene after 12 h[a]

| temp (°C) | $C_2H_4$ (psi) | ethyl benzene[b] | styrene[b] |
|---|---|---|---|
| 90 | 25 | none | none |
| 90 | 250 | 0.1 | trace |
| 90 | 500 | 0.1 | trace |
| 90 | 900 | 0.1 | trace |
| 150 | 500 | 0.4 | 1.0 |
| 150 | 800 | 0.4 | 1.2 |
| 180 | 500 | 2.2 | 0.9 |
| 180 | 800 | 3.6 | 2.5 |

[a] Butenes were also detected for the reactions (see below). [b] Given in TONs (turnover numbers) based on **2**.

***Chart 1.*** Coupling Constants for the $\eta^3$-Allyl Ligand of TpRu(PMe$_3$)($\eta^3$-C$_4$H$_7$) (**5**) Determined by Homonuclear Decoupling Experiments

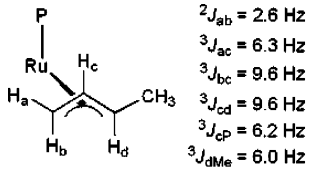


ethylene pressure of 80 psi results in a slightly reduced yield of **5**; see below). $^1$H NMR spectroscopy reveals five unique resonances consistent with the formation of the $\eta^3$-allyl ligand. Chart 1 displays coupling constants for the allyl protons, which were deduced using homonuclear decoupling experiments (see Experimental Section for more detailed information). A single-crystal X-ray diffraction study produced a structure that confirms the atom connectivity of **5**; however, the structure suffers from disorder likely due to the asymmetric nature of the allyl ligand.

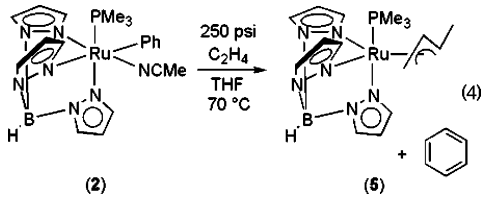


Using high-pressure J-Young NMR tubes, the conversion of **2** and ethylene (80 psi) to **5** was monitored at 60 °C in THF-$d_8$. During the conversion, the disappearance of **2**, the emergence and disappearance of three *primary* intermediates,[61] and the appearance of **5** were observed. The formation of **5** occurs with $t_{1/2} \sim 41$ h in approximately 90% yield. In contrast to higher pressures (i.e., 250 psi) of ethylene (see above), minor decomposition (~10−15%) is observed during the reaction using 80 psi of ethylene. On the basis of $^1$H NMR spectroscopy, the three primary intermediates are proposed to be TpRu(PMe$_3$)($\eta^2$-C$_2$H$_4$)Ph (**6**), TpRu(PMe$_3$)($\eta^2$-C$_2$H$_4$)($\eta^1$-C$_2$H$_3$) (**7**), and TpRu(PMe$_3$)($\eta^2$-C$_2$H$_4$)(CH$_2$CH$_2$CH=CH$_2$) (**8**) (Scheme 5). TpRu(PMe$_3$)(NCMe)($\eta^1$-C$_2$H$_3$) (**9**), which has been independently prepared and isolated, is also observed in very small amounts. Complex **6** has been independently prepared and isolated, while complex **7** has been independently generated and observed by $^1$H NMR spectroscopy but not isolated (see below and Experimental Section). The identity of **8** has not been confirmed by independent experiments and is indefinite (see below). Figure 6 depicts the concentration versus time plot for all species observed in the conversion of **2** and ethylene to **5** from a single experiment. Repetition of the kinetic analysis reveals similar plots (see Supporting Information).

Scheme 5 depicts a proposed pathway for the conversion of **2** and ethylene to the allyl complex **5**. TpRu(PMe$_3$)($\eta^2$-C$_2$H$_4$)Ph (**6**) is the first observed intermediate with resonances due to the coordinated ethylene (multiplets) at 3.15 and 2.77 ppm (THF-$d_8$). Consistent with the assignment of this species, monitoring the conversion of TpRu(PMe$_3$)(NCMe)($\eta^1$-C$_2$H$_3$) (**9**) and ethylene to the allyl complex **5** proceeds via **7** and **8** and does not involve the formation of **6** (see below). In addition, complex **6** has been independently prepared and characterized; however, due to decomposition in the absence of ethylene, clean elemental analysis of **6** was not possible (see Experimental Section). Ethylene C−H activation from **6** forms free benzene and the unobserved species TpRu(PMe$_3$)($\eta^1$-C$_2$H$_3$). Coordination of ethylene to TpRu(PMe$_3$)($\eta^1$-C$_2$H$_3$) forms TpRu(PMe$_3$)($\eta^2$-C$_2$H$_4$)($\eta^1$-C$_2$H$_3$) (**7**). By $^1$H NMR spectroscopy, the formation of **7** is accompanied by the production of free benzene. Complex **7** exhibits resonances at 8.19, 5.57, and 4.40 ppm, assigned to the vinyl ligand, and two multiplets at 2.85 and 2.44 ppm,

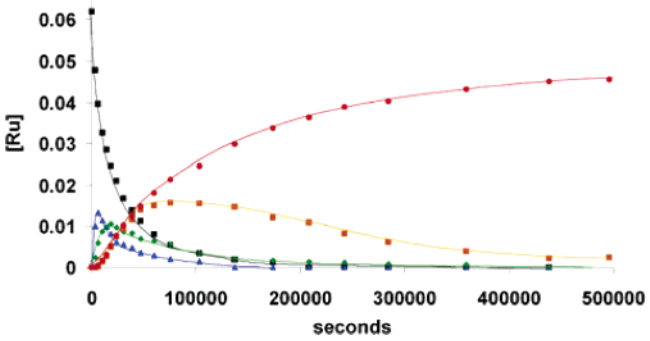


***Figure 6.*** Plot of concentration versus time for all species observed in the conversion of TpRu(PMe$_3$)(NCMe)Ph (**2**) and ethylene to TpRu(PMe$_3$)($\eta^3$-allyl) (**5**) including complex **2** (black, squares), **5** (red, circles), TpRu(PMe$_3$)($\eta^2$-C$_2$H$_4$)Ph (**6**) (blue, triangles), TpRu(PMe$_3$)($\eta^2$-C$_2$H$_4$)($\eta^1$-C$_2$H$_3$) (**7**) (green, diamonds), and TpRu(PMe$_3$)($\eta^2$-C$_2$H$_4$)(CH$_2$CH$_2$CH=CH$_2$) (**8**) (orange, squares). Data are from one experiment and were acquired at 60 °C in THF-$d_8$ under 80 psi of ethylene.

***Scheme 5.*** Proposed Mechanism for the Formation of TpRu(PMe$_3$)($\eta^3$-C$_4$H$_7$) (**5**) from the Reaction of TpRu(PMe$_3$)(NCMe)Ph (**2**) and Ethylene

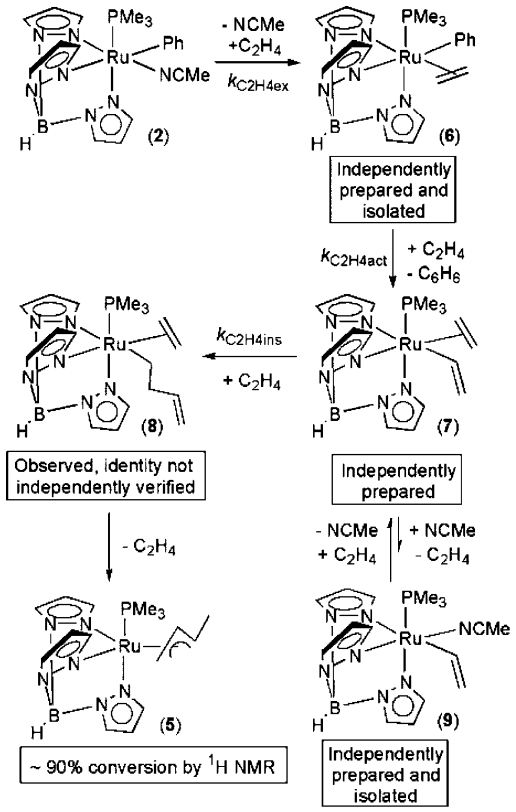


(61) Two other intermediates in less than 5% total abundance ($^1$H NMR spectroscopy) are observed and are presumed to be in equilibrium with complex **8**.

assigned to the coordinated ethylene. Insertion of ethylene into the Ru−vinyl bond of **7** and coordination of another 1 equiv of ethylene would produce complex **8**. Complex **8** is never present in large concentrations in the absence of multiple other Ru systems (later in the reaction, **8** is present in only low concentrations), and we have not independently produced this complex. Thus, establishing the structure of **8** is difficult, *and its identity is tentative*. Although it is reasonable to suggest complex **8** as TpRu($PMe_3$)($\eta^2$-$C_2H_4$)($CH_2CH_2CH{=}CH_2$), *all that can be confidently stated about **8** is that it is likely the precursor to the allyl complex **5**.*

Using kinetic simulation (using KINSIM/FITSIM software; see Supporting Information and Experimental Section) rate constants for the conversion of **2** to **5** were determined. The rate constant for the NCMe/ethylene ligand exchange [$k_{obs}$ = 1.9(4) × $10^{-4}$ $s^{-1}$] from TpRu($PMe_3$)(NCMe)Ph (**2**) is statistically identical with the rate of NCMe/$NCCD_3$ exchange for **2** ($k_{obs}$ = 1.5(1) × $10^{-4}$ $s^{-1}$) discussed above, which supports a dissociative pathway for both transformations. Assuming that ethylene coordination to TpRu($PMe_3$)($\eta^1$-$C_2H_3$) is rapid, the rate of conversion of **6** to **7** provides the rate of Ru-mediated ethylene C−H activation, which is estimated to be $k_{C_2H_4act}$ = 1.1(1) × $10^{-4}$ $s^{-1}$. Ethylene insertion into the Ru−vinyl bond of **7** forms TpRu($PMe_3$)($CH_2CH_2CH{=}CH_2$), which forms TpRu($PMe_3$)($\eta^2$-ethylene)($CH_2CH_2CH{=}CH_2$) (**8**) upon coordination of ethylene. Kinetic simulation suggests that ethylene insertion to form **8** occurs with $k_{C_2H_4ins}$ = 5.9(6) × $10^{-5}$ $s^{-1}$. The rate constant from kinetic simulation for ethylene insertion during the conversion of the vinyl complex TpRu($PMe_3$)(NCMe)($\eta^1$-$C_2H_3$) (**9**) and ethylene to **5** provides a check of $k_{C_2H_4ins}$ determined from the conversion of **2** and ethylene to **5**, and this value is 5.7(6) × $10^{-5}$ $s^{-1}$ (see below). Dissociation of ethylene from **8** and rearrangement of the butenyl ligand "$CH_2CH_2CH{=}CH_2$" likely leads to the formation of the allyl complex **5**.

The $\eta^1$-vinyl complex TpRu($PMe_3$)(NCMe)($\eta^1$-$C_2H_3$) (**9**) has been isolated in 66% yield upon reaction of TpRu($PMe_3$)(NCMe)OTf and Mg(vinyl)$_2$[diglyme]$_{1.5}$ and has been characterized by $^1$H, $^{13}$C, and $^{31}$P NMR spectroscopy as well as high-resolution mass spectrometry (eq 5). $^1$H NMR spectroscopy of

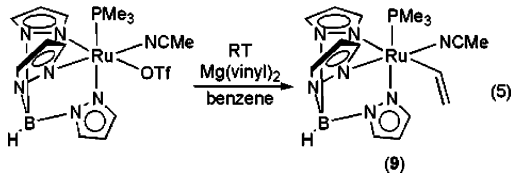


**9** shows 3 distinct downfield resonances (each ddd's) at 8.83 ppm (vinyl hydrogen α to Ru), 6.62 ppm ($\beta$ vinyl hydrogen trans to Ru), and 5.68 ppm ($\beta$ vinyl hydrogen cis to Ru). All vinyl resonances are coupled to the phosphorus of the $PMe_3$ ligand with 3.0, 1.7, and 1.1 Hz coupling constants, respectively. Relative to complex **9**, the $^1$H NMR spectrum of Mg(vinyl)$_2$[diglyme]$_{1.5}$ reveals resonances shifted upfield. Heating complex **9** at 70 °C in $C_6D_6$ produces **2**-$d_5$ and $C_2H_3D$ ($^1$H NMR spectroscopy) (eq 6). Additionally, reaction of **9** with HCl produces free $C_2H_4$ ($^1$H NMR spectroscopy) and TpRu($PMe_3$)(NCMe)Cl (**10**) (eq 7). To verify the identity of **10**, this complex has been independently synthesized and characterized including a single-crystal solid-state X-ray diffraction study (see Experimental Section and Supporting Information).

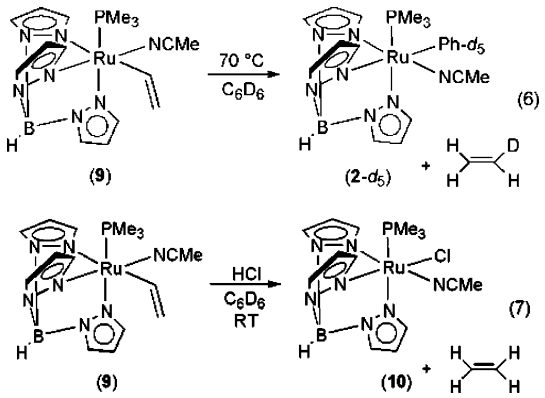


Consistent with TpRu($PMe_3$)($\eta^1$-$C_2H_3$) being an intermediate in the conversion of **2** and ethylene to **5**, heating complex **9** under 80 psi of ethylene at 60 °C in THF-$d_8$ (high-pressure J-Young tube) results in the complete conversion to complex **5** with a half-life of approximately 21.5 h (eq 8). Similar to the reaction of **2** and ethylene to produce the allyl complex **5**, during the conversion of **9** and ethylene to **5**, $^1$H NMR spectroscopy shows the presence of TpRu($PMe_3$)($\eta^2$-$C_2H_4$)($\eta^1$-$C_2H_3$) (**7**), and the rate of conversion of **7** to complex **8** ($k_{C_2H_4ins}$ = 5.7(6) × $10^{-5}$ $s^{-1}$) from this experiment is consistent with the rate of the same reaction determined during the conversion of **2** and ethylene to complex **5** (see above).

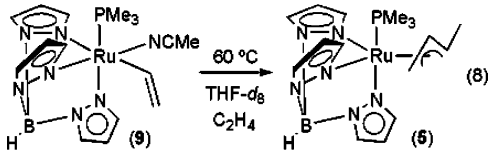


Similar to **2**, during catalytic hydrophenylation of ethylene using complex **1**, at *prolonged* reaction times and *high* ethylene pressures, the allyl complex TpRu(CO)($\eta^3$-$C_4H_7$) (**11**) is formed. At 250 psi of ethylene in THF at 70 °C, complex **1** is converted to **11** in 98% isolated yield. Monitoring the conversion of **1** to **11** by $^1$H NMR spectroscopy in THF-$d_8$ at 60 °C at 80 psi of ethylene (Figure 7) reveals substantial differences from the conversion of the $PMe_3$ complex **2** and ethylene to **5**. Com-

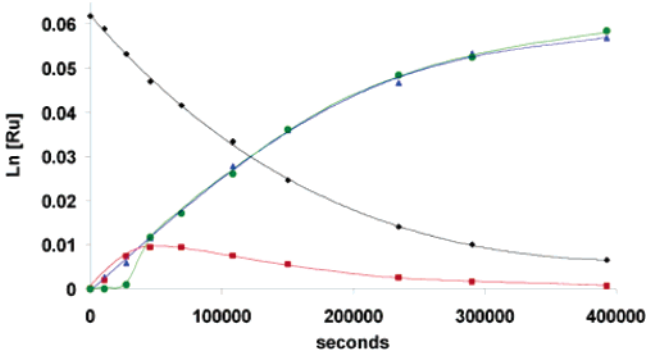


***Figure 7.*** Plot of concentration versus time for all species observed in the conversion of TpRu(CO)(NCMe)Ph (**1**) and ethylene to TpRu(CO)($\eta^3$-allyl) (**11**) including complex **1** (black, squares), TpRu(CO)($\eta^2$-$C_2H_4$)($CH_2CH_2$-Ph) (red, squares), ethylbenzene (blue, triangles), and complex **11** (green, circles). Data are from one experiment and were acquired at 60 °C in THF-$d_8$ under 80 psi of ethylene.

***Scheme 6.*** Proposed Pathway for Conversion of TpRu(CO)(NCMe)Ph (**1**) and Ethylene to the Allyl Complex TpRu(CO)($\eta^3$-$C_4H_7$) (**11**)

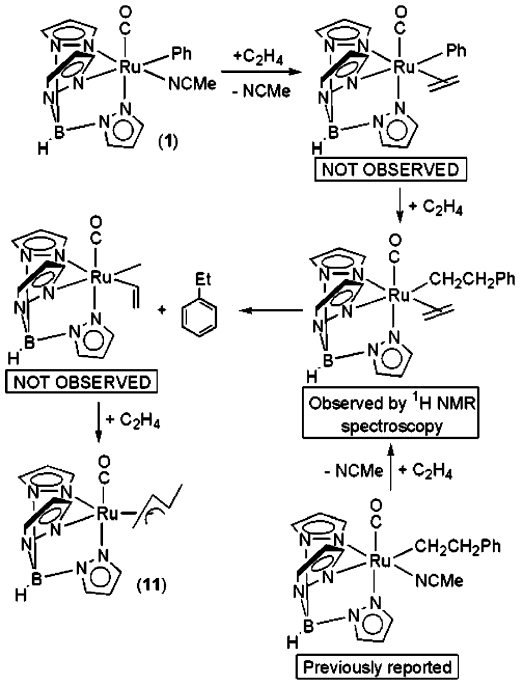


parison of the rates of disappearance of TpRu(CO)(NCMe)Ph (**1**) and TpRu($PMe_3$)(NCMe)Ph (**2**) under ethylene pressure indicates that the rate of exchange of NCMe for $C_2H_4$ by complex **2** [$k_{obs} = 1.9(4) \times 10^{-4}$ $s^{-1}$; see above] is approximately 30 times more rapid than that of complex **1** [$k_{obs} = 6.1(2) \times 10^{-6}$ $s^{-1}$, taken from kinetic simulation of conversion of **1** to TpRu(CO)($\eta^2$-$C_2H_4$)($CH_2CH_2Ph$), for which the RDS is likely dissociation of NCMe]. The reaction of TpRu($PMe_3$)(NCMe)Ph (**2**) and ethylene initially produces TpRu($PMe_3$)($\eta^2$-$C_2H_4$)Ph (**6**), which subsequently converts to TpRu($PMe_3$)($\eta^2$-$C_2H_4$)($\eta^1$-$C_2H_3$) and *free benzene*. *In contrast*, the reaction of TpRu(CO)(NCMe)Ph (**1**) and ethylene does not produce observable TpRu(CO)($\eta^2$-$C_2H_4$)Ph. Rather, the first observed species by $^1$H NMR spectroscopy is assigned as TpRu(CO)($\eta^2$-$C_2H_4$)($CH_2CH_2Ph$). Consistent with this assignment, the reaction of previously reported TpRu(CO)(NCMe)($CH_2CH_2Ph$) with ethylene (THF-$d_8$) at 60 °C produces the same complex (followed by formation of the allyl complex **11**). The production of *ethylbenzene* (observed by $^1$H NMR spectroscopy and confirmed by GC/MS) occurs simultaneous with the conversion of TpRu(CO)($\eta^2$-$C_2H_4$)($CH_2CH_2Ph$) to complex **11**. No evidence for the formation of free benzene is obtained. The formation of TpRu(CO)($\eta^3$-$C_4H_7$) (**11**) is quantitative with $t_{1/2} \sim 34$ h. These observations are consistent with relatively rapid insertion of ethylene into the Ru−Ph bond of TpRu(CO)($\eta^2$-$C_2H_4$)Ph to form TpRu(CO)($CH_2CH_2Ph$), which coordinates ethylene to produce TpRu(CO)($\eta^2$-$C_2H_4$)($CH_2CH_2Ph$). Carbon−hydrogen bond activation of coordinated ethylene produces ethylbenzene and an unobserved Ru−vinyl complex, which rapidly converts in the presence of ethylene to the allyl complex **11** (Scheme 6). Simulation of the kinetic data reveals that the rate of ethylene C−H activation by TpRu(CO)($\eta^2$-$C_2H_4$)($CH_2CH_2Ph$) is $k_{C_2H_4act} = 3.4(4) \times 10^{-5}$ $s^{-1}$ [assuming that the RDS for the formation of **11** from TpRu(CO)($\eta^2$-$C_2H_4$)($CH_2CH_2Ph$) is ethylene C−H activation]. In comparison, the rate of ethylene C−H activation by TpRu($PMe_3$)($\eta^2$-$C_2H_4$)Ph (**6**) is simulated to be $k_{C_2H_4act} = 1.1(1) \times 10^{-4}$ $s^{-1}$, which is approximately 3 times more rapid than the CO system. Thus, the relative rates of olefin C−H activation are similar to the relative rates of overall benzene C−H(D) activation by TpRu(CO)(Ph)(benzene) and TpRu($PMe_3$)(Ph)(benzene) systems with the $PMe_3$ system initiating C−H activation ~3 times more rapidly than the CO complex (see Table 2).

***Table 4.*** Hydrovinylation Catalysis Results for TpRu($PMe_3$)($\eta^3$-$C_4H_7$) (**5**) and TpRu(CO)($\eta^3$-$C_4H_7$) (**11**)[a]

| catal | $C_2H_4$ (psi) | temp (°C) | butenes[b] | hexenes[b] |
|---|---|---|---|---|
| 5 | 150 | 180 | 0.4 | 0.6 |
| 5 | 300 | 180 | 2.0 | 1.0 |
| 5 | 600 | 180 | 4.4 | 2.3 |
| 5 | 800 | 180 | 3.9 | 2.3 |
| 11 | 600 | 180 | 0.9 | 5.5 |
| 11 | 800 | 180 | 0.8 | 5.0 |

[a] Organic products were a mixture of various isomers. [b] Given in TONs based on **5** or **11**.

**Catalytic Hydrovinylation of Ethylene.** The catalytic hydrovinylation of ethylene using allyl complex **5** was studied under variable conditions. Complex **5** was placed under ethylene pressure in mesitylene and heated to 180 °C, and aliquots were withdrawn for GC/MS analysis, which revealed mixtures of 1-butene, *cis*-butene, *trans*-butene, and various isomers of hexene (Table 4). The three butene isomers were partially resolved (but not fully separated) by GC-MS, and the approximate molar ratio of 1-butene, *cis*-butene, and *trans*-butene was 1:1:1, which is only marginally variable with reaction condition. Isomers of hexene were not separated by GC-MS. The CO allyl complex TpRu(CO)($\eta^3$-$C_4H_7$) (**11**) also catalyzes ethylene hydrovinylation and oligomerization. Consistent with the more rapid rate of ethylene insertion for CO versus $PMe_3$ systems (see below), the CO allyl complex **11** results in the predominant formation of hexenes (relative to butenes). Periana et al. have reported catalytic hydrovinylation of olefins by closely related Ir(III) systems.[62,63]

**Computational Studies: Comparison of Overall Catalytic Cycle for Hydrophenylation of Ethylene.** We have used computational studies to probe four transformations: (1) catalytic hydrophenylation of ethylene by TpRu(L)(NCMe)Ph; (2) benzene C−H activation by TpRu(L)(NCMe)Ph; (3) ethylene insertion from TpRu(L)($\eta^2$-$C_2H_4$)Ph; (4) ethylene C−H activation from TpRu(L)($\eta^2$-$C_2H_4$)Ph. The energetics of the steps anticipated to be involved in the catalytic hydrophenylation of ethylene were calculated for both TpRu(L)(NCMe)Ph (L = CO or $PMe_3$) systems including transition states for ethylene insertion into the Ru−Ph bond and benzene C−H activation (Scheme 7). For each coligand, the highest energy species is calculated to be the transition state for benzene C−H activation starting from TpRu(L)($\eta^2$-benzene)($CH_2CH_2Ph$). From the starting complex TpRu(L)(NCMe)Ph, the overall reaction barrier is calculated to be 30.9 kcal/mol for L = CO, while the activation barrier is calculated to be higher at 40.1 kcal/mol for L = $PMe_3$. Thus, the calculations indicate that the benzene C−H activation event by the phenethyl complex is the rate-determining step for both CO and $PMe_3$ coligands. This result is

(62) Oxgaard, J.; Bhalla, G.; Periana, R. A.; Goddard, III, W. A. *Organometallics* **2006**, *25*, 1618−1625.
(63) Bhalla, G.; Oxgaard, J.; Goddard, W. A.; Periana, R. A. *Organometallics* **2005**, *24*, 5499−5502.

***Scheme 7.*** Calculated Gibbs Free Energy (kcal/mol; 298 K) for Proposed Steps in the Catalytic Hydrophenylation of Ethylene by TpRu(L)(NCMe)Ph (L = CO or $PMe_3$)

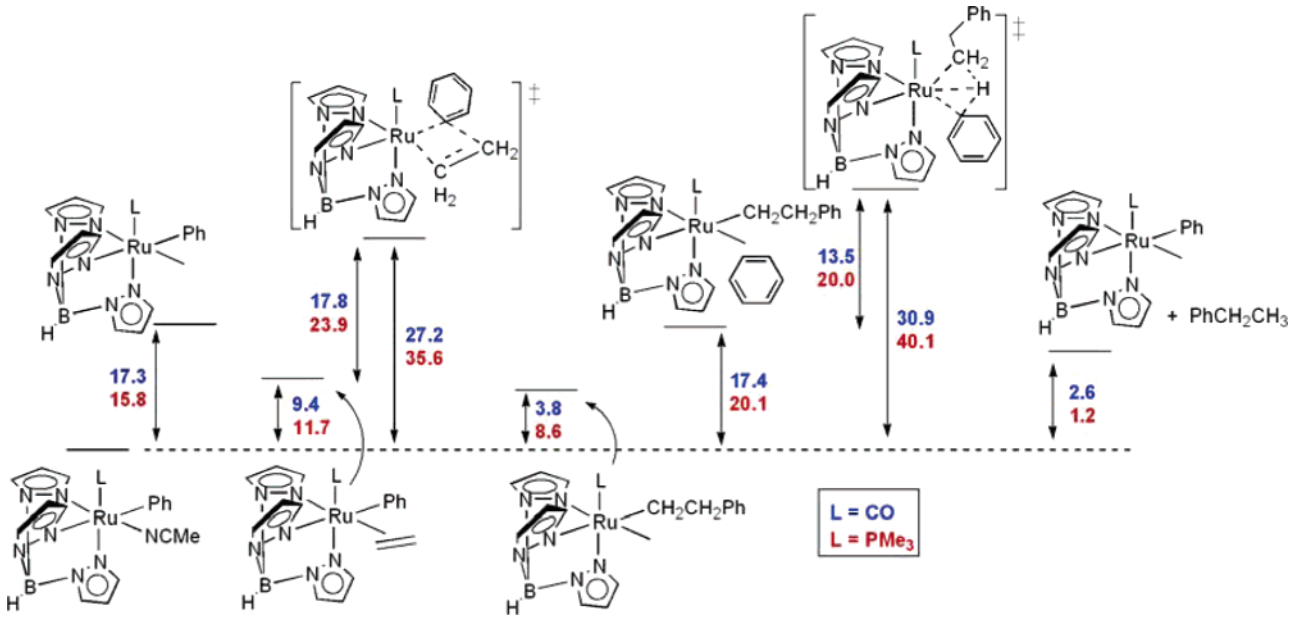


***Scheme 8.*** Calculated Gibbs Free Energy (kcal/mol; 298 K) for Benzene C−H Activation by TpRu(L)(NCMe)Ph (L = CO, $PMe_3$, CNH, or $PEt_3$)

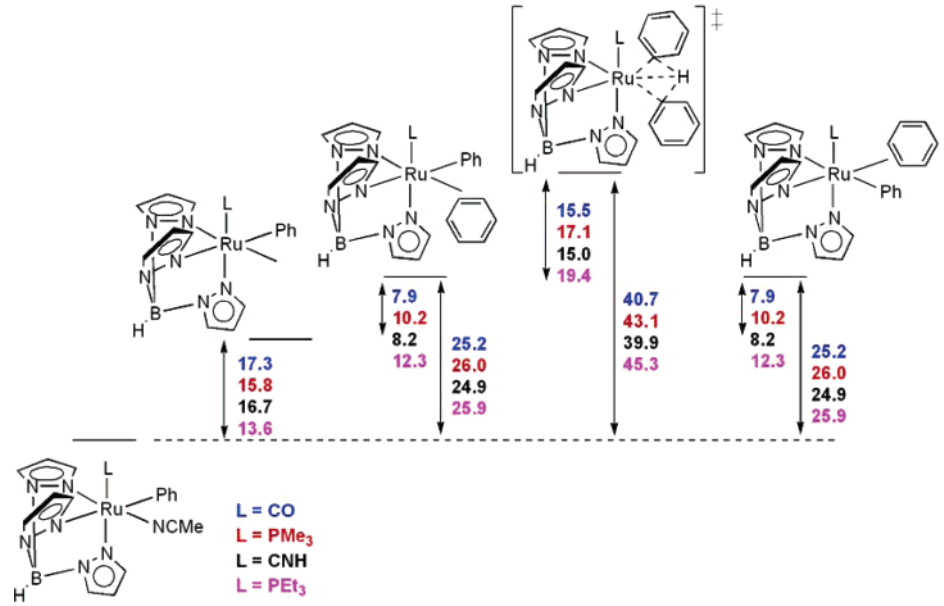


consistent with the observation of intermolecular kinetic isotope effects for the catalytic hydrophenylation of ethylene by TpRu(CO)(NCMe)Ph.[45] In view of the more similar calculated C−H activation barriers for the less hindered TpRu(L)(benzene)Ph systems discussed in the following section, we propose that the larger difference in $\Delta G^{\ddagger}$ for benzene C−H activation by TpRu(L)(benzene)($CH_2CH_2Ph$) systems is due primarily to steric hindrance between the $CH_2CH_2Ph$ ligand and $PMe_3$ (see below for a discussion on the possible influence of sterics on C−H activation).

**Computational Studies: Comparison of Benzene C−H Activation.** Benzene C−H activation by TpRu(L)Ph is a degenerate reaction and thus provides an opportunity to assess the intrinsic kinetic influence of L = $PMe_3$ versus L = CO. The first step in the proposed pathway for benzene activation is the loss of acetonitrile from 18-electron TpRu(L)(NCMe)-Ph. This reaction is calculated to be endergonic by 15.8 kcal/mol for L = $PMe_3$. This is more favorable than acetonitrile loss for L = CO, which is endergonic by 17.3 kcal/mol (Scheme 8). Although the calculated energetics for nitrile loss are ground-state values, the trend is consistent with the dissociative ligand exchange of NCMe (with $NCCD_3$ or ethylene) of the $PMe_3$ complex **2** being more rapid than for the CO complex **1** (see above). The strongly $\pi$-acidic CO may increase the Lewis acidity of TpRu(CO)R relative to the more electron-rich TpRu($PMe_3$)R systems and, hence, render dissociation of the Lewis base NCMe less facile from **1**.

Acetonitrile loss is followed by benzene coordination to the 16-electron intermediates TpRu(L)Ph. While benzene ligation is calculated to be mildly exothermic ($\Delta H$ is calculated to be negative), the introduction of an unfavorable entropy term makes the binding of benzene endergonic ($\Delta G$ is calculated to be

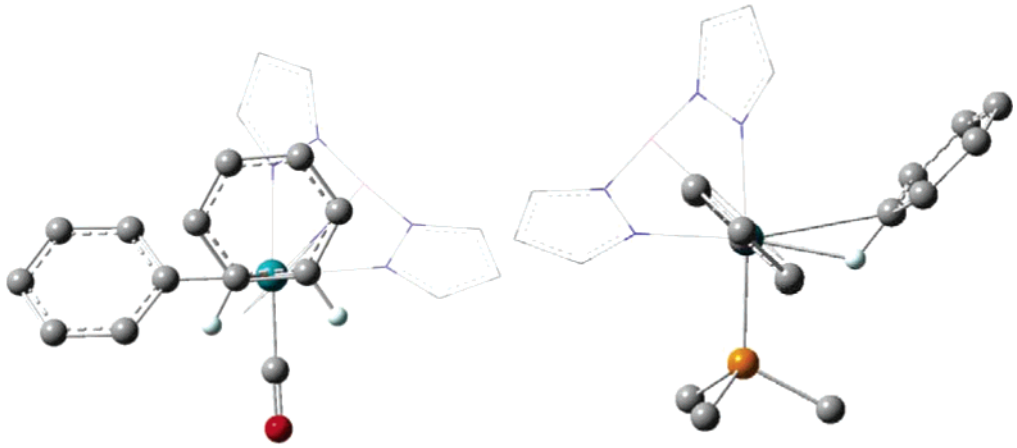

***Figure 8.*** Calculated benzene adduct geometries of TpRu(L)(Ph)($C_6H_6$) for L = CO (left) and L = $PMe_3$ (right). Most hydrogen atoms are omitted for clarity. The Tp ligand is shown in wire frame.

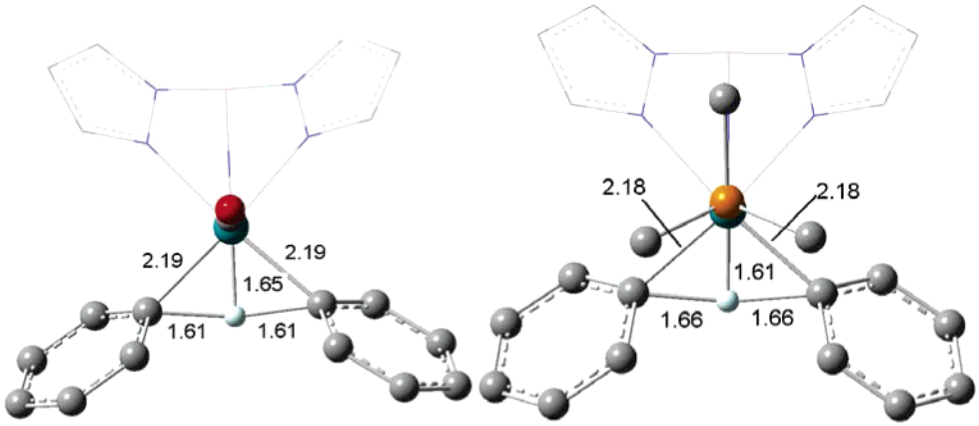


***Figure 9.*** Comparison of calculated transition states for benzene C−H activation by TpRu(L)(benzene)Ph (L = CO, shown on left, or $PMe_3$, shown on right).

positive) by +10.2 kcal/mol for L = $PMe_3$ and +7.9 kcal/mol for L = CO (Scheme 8). An interesting dichotomy in structure is seen for the calculated benzene adducts; while the carbonyl complex is an $\eta^2$-C═C adduct, the trimethylphosphine complex is an agostic $\eta^2$-C−H adduct (Figure 8). This may reflect a steric inhibition against $\eta^2$-C═C coordination of benzene to the TpRu($PMe_3$)Ph fragment, thus explaining the less favorable binding of benzene to TpRu($PMe_3$)Ph versus TpRu(CO)Ph.

To compare steric versus electronic effects for benzene coordination and C−H activation, we calculated the energetics of these transformations for TpRu(C≡NH)(NCMe)Ph. It is anticipated that the isonitrile complex will sterically resemble TpRu(CO)(NCMe)Ph (**1**) but will be more similar electronically to TpRu($PMe_3$)(NCMe)Ph (**2**) due to the strong $\sigma$-donor nature of the isonitrile ligand. Consistent with the hypothesis that the $\eta^2$-C−H coordination mode of TpRu($PMe_3$)(benzene)Ph results from *steric influence* of the phosphine ligand, the benzene ligand of TpRu(C≡NH)(benzene)Ph is calculated to be coordinated $\eta^2$-C═C and is thus akin to the carbonyl congener.

For L = $PMe_3$, the calculated benzene C−H activation barrier is 17.1 kcal/mol (relative to the benzene adduct). Replacing the $PMe_3$ ligand with carbon monoxide is calculated to *lower* the activation barrier by 1.6 kcal/mol to 15.5 kcal/mol (Scheme 8). Consistent with the small difference in calculated $\Delta G^{\ddagger}$'s, there is little difference in the calculated transition state geometries for benzene C−H activation by TpRu(L)Ph as a function of L as is evident from Figure 9. For the overall C−H activation of benzene starting from TpRu(L)(NCMe)Ph complexes, the calculations reveal that the $\Delta G^{\ddagger}$ for L = CO (40.7 kcal/mol) is lower than $PMe_3$ (43.1 kcal/mol) with $\Delta\Delta G^{\ddagger}$ = 2.4 kcal/mol.

The calculated energetics of benzene C−H activation for the parent isonitrile system relative to the CO and $PMe_3$ systems are revealing (Scheme 8). Relative to the benzene adduct TpRu(C≡NH)($\eta^2$-benzene)Ph, the calculated activation barrier for benzene C−H activation is 15.0 kcal/mol, which is lower than either the CO (15.5 kcal/mol) and $PMe_3$ (17.1 kcal/mol) systems. Likewise, the calculated overall barrier for starting from TpRu(C≡NH)(NCMe)Ph (39.9 kcal/mol) is lower than the barriers calculated for the CO (40.7 kcal/mol) and $PMe_3$ (43.1 kcal/mol) complexes. These results suggest that the electronic influence of ligand "L" of TpRu(L) systems on the activation barriers of benzene C−H activation is relatively small, with more electron-donating ligands *slightly* reducing the free energy of activation (compare CO versus C≡NH systems); however, steric influence (vis-à-vis the $PMe_3$ system) can have as substantial an influence on the energetics as electronic factors. Given the proposed role of sterics for C−H activation, the larger difference in calculated $\Delta G^{\ddagger}$'s for benzene C−H activation by the phenethyl complexes TpRu(L)(benzene)($CH_2CH_2Ph$) (L = CO, $PMe_3$; $\Delta\Delta G^{\ddagger}$ = 6.5 kcal/mol, see Scheme 7) compared with benzene C−H activation by TpRu(L)(benzene)Ph likely

***Scheme 9.*** Calculated Reaction Coordinate for C−H Activation of Ethylene by TpRu(L)Ph for L = $PMe_3$ (red) and L = CO (blue)[a]

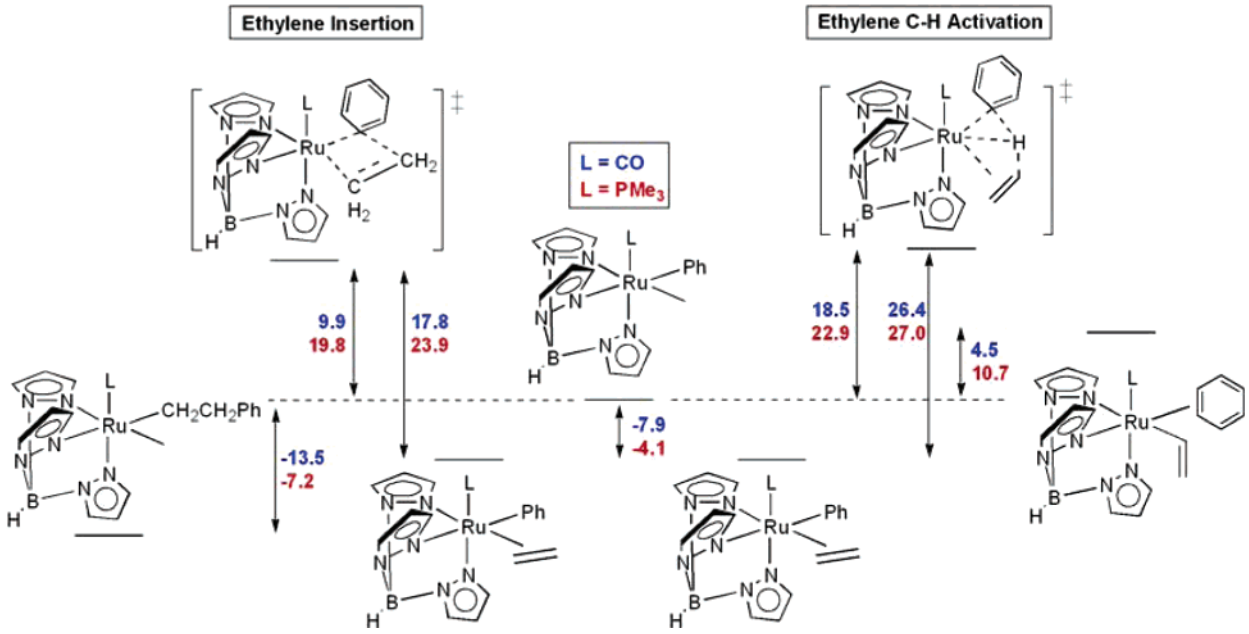


[a] The calculated free energies (in kcal/mol; 298 K) indicated for each stationary point are relative to separated ethylene and TpRu(L)Ph.

reflects the increased steric impact due to the $sp^3$-methylene group of the phenethyl ligand in place of the planar phenyl ring.

To confirm the proposed role of steric influence of "L" on benzene C−H activation, we have calculated the energetics for TpRu($PEt_3$)(NCMe)Ph, which is electronically similar to **2** but sterically more imposing (Scheme 8). Consistent with the proposed impact of the steric profile of ancillary ligand "L", benzene C−H activation by TpRu($PEt_3$)(NCMe)Ph is calculated to have a higher energy barrier than for the analogous $PMe_3$ system. From the benzene adduct TpRu(L)(benzene)Ph, the $\Delta G^{\ddagger}$ for benzene C−H activation is 19.4 kcal/mol for L = $PEt_3$ compared to 17.1 kcal/mol for L = $PMe_3$. Likewise, the overall activation barrier for benzene C−H activation starting from TpRu($PEt_3$)(NCMe)Ph (calculated $\Delta G^{\ddagger}$ = 45.3 kcal/mol) is more substantial than the calculated overall barrier starting from TpRu($PMe_3$)(NCMe)Ph (calculated $\Delta G^{\ddagger}$ = 43.1 kcal/mol).

**Computational Studies: Comparison of Ethylene C−H Activation and Ethylene Insertion.** The reaction coordinates for C−H activation of ethylene by TpRu(L)($\eta^2$-$C_2H_4$)Ph were calculated for both L = CO and L = $PMe_3$ (Scheme 9). Unlike the benzene substrate, ethylene binds favorably to the 16-electron TpRu(L)(Ph) intermediate. For L = $PMe_3$, the calculated ethylene binding free energy ($\Delta G_{bind}$) is −4.1 kcal/mol. Similar to the impact of CO/$PMe_3$ substitution on relative affinities for NCMe coordination to TpRu(L)Ph, replacing $PMe_3$ with CO results in an enhancement in $C_2H_4$ binding with $\Delta G_{bind}$ = −7.9 kcal/mol. Calculated activation barriers for ethylene C−H activation relative to the $\eta^2$-ethylene adducts, $\Delta G^{\ddagger}_{act}$ = 27.0 kcal/mol (L = $PMe_3$) and 26.4 kcal/mol (L = CO), are high compared to benzene C−H activation, which are 17.1 and 15.5 kcal/mol, respectively. Given the commensurate carbon−hydrogen BDEs for benzene (∼113 kcal/mol[64]) and ethylene (∼111 kcal/mol[64]), the greater C−H activation barriers for the latter partially reflect the greater thermodynamic stability of the TpRu(L)($\eta^2$-$C_2H_4$)Ph precursor versus the corresponding benzene adducts. Of course, one must consider the different driving forces for C−H bond scission for each spectator ligand. As expected from the Hammond postulate, there is a correlation between a higher kinetic barrier and lower thermodynamic driving force. Calculated reaction free energies {TpRu(L)($\eta^2$-$C_2H_4$)Ph to TpRu(L)($\eta^1$-$C_2H_3$)($\eta^2$-$C_6H_6$)} are $\Delta G_{rxn}$ = +14.8 kcal/mol (L = $PMe_3$), +12.4 kcal/mol (L = CO) (Scheme 9), while analogous reactions for benzene C−H activation are, of course, thermoneutral.

In the active site of the ethylene C−H activation transition states there are structural distinctions that hint at differences engendered by the disparate electronic and steric demands of CO versus $PMe_3$ (Figure 10). A comparison of the calculated geometries, Figure 10, shows little difference in the Ru···C distances of the four-center transition states but a more noticeable shift in the position of the activated hydrogen: $C_{vy}$···H = 1.55 Å (CO), 1.62 Å ($PMe_3$); Ru···H = 1.67 Å (CO), 1.62 Å ($PMe_3$). Perhaps the most intriguing difference in the transition state geometries is the observation that the $PMe_3$ complex has a distinctly nonplanar geometry active site with $\tau$($C_{vy}$···H···$C_{Ph}$···Ru) = 16° versus 5° for L = CO complex. This is unusual for four-centered, C−H bond activation transition states and potentially suggests greater steric pressure for the $PMe_3$ ancillary ligand versus CO. From thermodynamic and kinetic considerations, the calculations imply a slightly more potent ethylene C−H activation system for TpRu(CO)(Ph) than TpRu($PMe_3$)(Ph), although the calculated magnitude of $\Delta\Delta G^{\ddagger}$ (∼1 kcal/mol) is small.

Calculations on the reactions of ethylene and TpRu(L)Ph indicate kinetic and thermodynamic advantages for C═C insertion versus ethylene C−H bond activation. This is not surprising given the former involves the investment of a C═C $\pi$-bond (energy ∼65 kcal/mol[65,66]) while the latter requires

(64) Afeefy, Y.; Liebman, J. F.; Stein, S. E. Neutral Thermochemical Data. In *NIST Chemistry WebBook*; NIST: Washington, DC, 2005.

(65) Douglas, J. E.; Rabinovitch, B. S.; Looney, F. S. *J. Chem. Phys* **1955**, *23*, 315−323.

(66) Nicolaides, A.; Borden, W. T. *J. Am. Chem. Soc.* **1991**, *113*, 6750−6755.

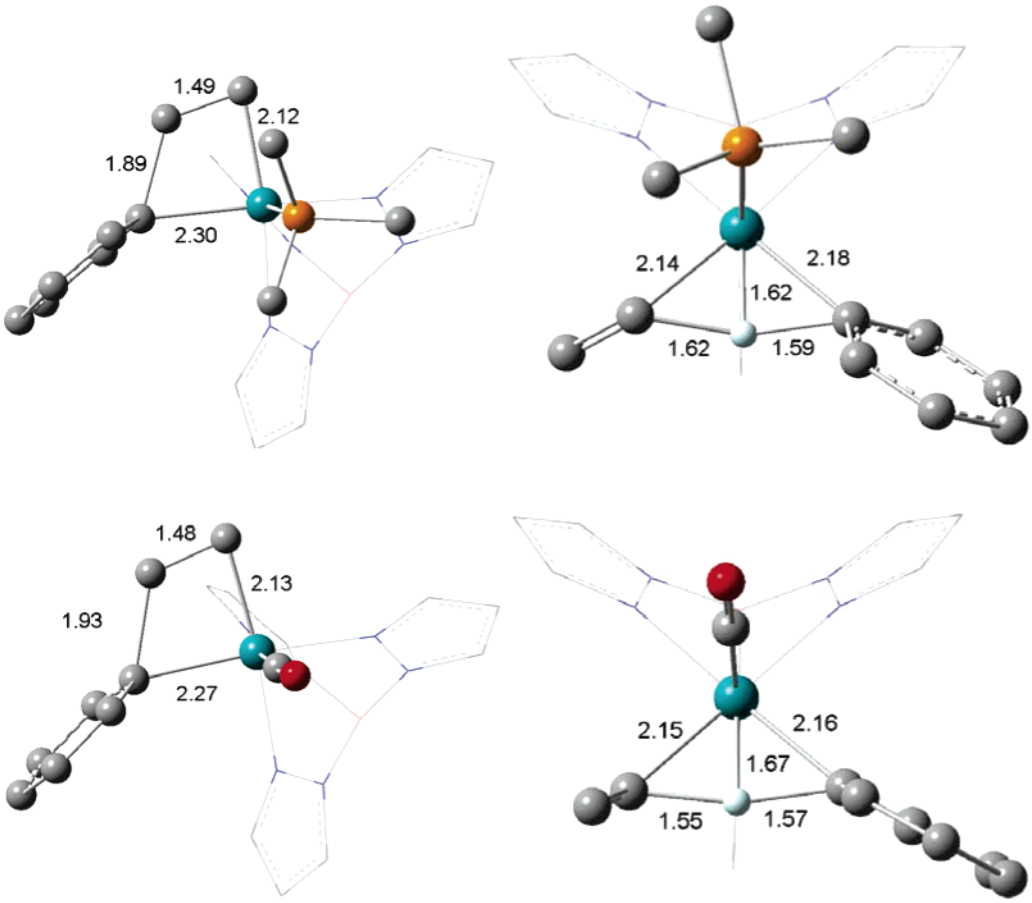


***Figure 10.*** Calculated bond lengths (Å) of active site in transition states for ethylene C−H activation (right) and ethylene insertion (left) by TpRu(L)(Ph) for L = CO (bottom) and L = $PMe_3$ (top).

scission of a strong, vinylic C−H bond (BDE ∼111 kcal/mol[64]). What is more interesting are the calculated differences in the selectivity between these pathways engendered by alteration of the spectator ligand from L = $PMe_3$ to L = CO. Ethylene insertion by the $PMe_3$ complex is calculated to be exergonic by 3.1 kcal/mol relative to the ethylene adduct, while ethylene insertion for the CO complex is calculated to be exergonic by 5.6 kcal/mol (Scheme 9). There is a substantial difference in the calculated $\Delta G^{\ddagger}$'s for ethylene insertion into the Ru−Ph bond of TpRu(L)($\eta^2$-$C_2H_4$)Ph, which are 17.8 kcal/mol (L = CO) and 23.9 kcal/mol (L = $PMe_3$). Thus, from TpRu(L)($\eta^2$-$C_2H_4$)-Ph systems, the calculated $\Delta\Delta G^{\ddagger}$ for ethylene insertion for L = CO vs $PMe_3$ is 6.1 kcal/mol while the calculated $\Delta\Delta G^{\ddagger}$ for ethylene C−H activation (0.6 kcal/mol) and benzene C−H activation [1.6 kcal/mol; from TpRu(L)(benzene)Ph] are substantially smaller (Schemes 8 and 9). *Thus, for TpRu(L)Ph systems, the calculations suggest that substitution of $PMe_3$ for CO has a more dramatic impact on the rate of ethylene insertion than either ethylene or benzene C−H activation steps.*

## Discussion

Previous experimental and computational studies of catalytic olefin hydroarylation by TpRu(CO)(NCMe)R complexes have indicated that the RDS for the catalytic cycle is the aromatic C−H activation step.[45] Calculations suggest that the transition state for the aromatic C−H activation may possess "oxidative" character and might be aided by the interaction between Ru and the hydrogen atom being activated.[45,54] Formal substitution of CO with $PMe_3$ provides TpRu($PMe_3$)(NCMe)R complexes, which were anticipated to exhibit increased electron density relative to TpRu(CO)(NCMe)R systems. Consistent with the expected increase in Ru-based electron density upon formal substitution of CO with $PMe_3$, cyclic voltammetry reveals that the Ru(III/II) redox potentials for the $PMe_3$ phenyl and methyl complexes **2** and **3**, respectively, are 0.30 and 0.10 V (versus NHE), respectively, while the corresponding potentials for TpRu(CO)(NCMe)Ph and TpRu(CO)(NCMe)Me are 1.03 and 0.95 V.[44]

Reactions of TpRu(L)(NCMe)Ph (L = CO or $PMe_3$) with $C_6D_6$ reveal that overall benzene C−H(D) activation is approximately 2−3 times more rapid (depending on concentration of NCMe; see Table 2) when L = $PMe_3$; however, calculations suggest that the $\Delta G^{\ddagger}$ for benzene C−H activation from TpRu-(L)(benzene)Ph is actually lower for L = CO than L = $PMe_3$, a prediction that is counter to experimental observations. However, both experimental results and calculations suggest that the difference in Gibbs free energy for benzene C−H activation by TpRu(L)(NCMe)Ph systems upon formal substitution of CO with $PMe_3$ is small. In addition, the calculated energetics are for gas-phase reactions. Perhaps more important than a precise match of experimental and computational results where the experimental difference in Gibbs free energy for the two reactions is likely <1 kcal/mol is that while CO/$PMe_3$ substitution influences the overall rate of benzene activation by TpRu-(L)(benzene)Ph, the impact is relatively minor with <1 kcal/

***Table 5.*** Comparison of Calculated $\Delta G^{\ddagger}$ Values (298 K, kcal/mol) for Ethylene Insertion, Ethylene C−H Activation of Benzene C−H Activation[a]

| reaction | CO | $PMe_3$ | $\Delta\Delta G^{\ddagger}$ |
|---|---|---|---|
| ethylene insertion | 27.2 | 35.6 | 8.4 |
| ethylene C−H activation | 35.8 | 38.7 | 2.9 |
| benzene C−H activation | 40.7 | 43.1 | 2.4 |

[a] All $\Delta G^{\ddagger}$ values are reported relative to TpRu(L)(NCMe)Ph starting complexes.

***Scheme 10.*** TpRu(L)(NCMe)Ph Kinetic Competition between Olefin Insertion and Olefin C−H Activation[a]

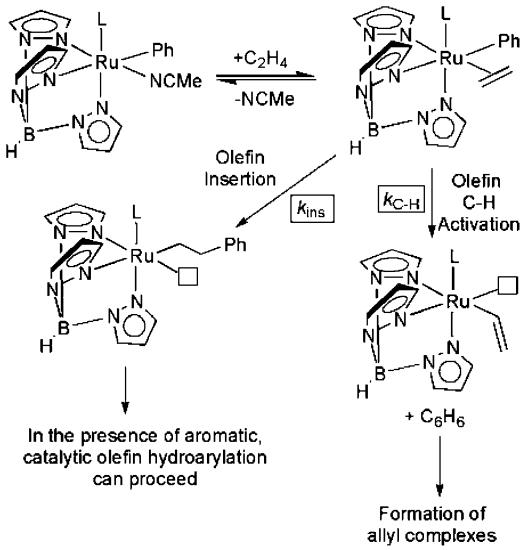


$k_{ins}/k_{C\text{-}H}$ for L = CO > $k_{ins}/k_{C\text{-}H}$ for L = $PMe_3$

[a] For L = CO, $k_{ins}$ outcompetes $k_{C-H}$. For L = $PMe_3$, $k_{C-H}$ becomes competitive with $k_{ins}$.

mol difference from experiment and only 2.4 kcal/mol difference (overall reaction) from calculations.

Despite the increased facility of benzene C−H activation, the $PMe_3$ complex **2** is a much poorer catalyst for the hydrophenylation of olefins than complex **1**. For example, at 90 °C and 25 psi of ethylene, **1** catalyzes the formation of ethylbenzene with approximately 50 turnovers after 4 h. In contrast, optimal results for **2** yield only 3.6 turnovers of ethylbenzene production at 180 °C and 800 psi of ethylene in 12 h. Furthermore, while **1** catalyzes the hydrophenylation of α-olefins (e.g., 1-hexene), **2** shows no activity for the hydrophenylation of these substrates. Closer scrutiny of the catalytic reactions using **2** reveals complications. Complex **2** reacts with ethylene to initiate olefin C−H activation to produce free benzene and a Ru−vinyl system, which converts to the $\eta^3$-allyl complex **5** in the presence of excess ethylene (Scheme 5). Likewise, the CO complex **1** reacts with ethylene to produce the $\eta^3$-allyl complex **11**; however, in contrast to the pathway for the formation of the $PMe_3$ allyl complex **11**, the reaction of **1** with ethylene (in the absence of benzene) proceeds via ethylene coordination *and relatively rapid olefin insertion*, which is followed by ethylene C−H activation to produce free ethylbenzene and, ultimately, the $\eta^3$-allyl complex **11** (Scheme 6). Calculations are consistent with the more rapid insertion of ethylene into the Ru−Ph bond of TpRu(CO)($\eta^2$-$C_2H_4$)Ph versus ethylene C−H activation with a calculated $\Delta G^{\ddagger}$ of 17.8 kcal/mol for ethylene insertion and a calculated $\Delta G^{\ddagger}$ of 26.4 kcal/mol ($\Delta\Delta G^{\ddagger}$ = 8.6 kcal/mol) for ethylene C−H activation. In contrast, the calculated $\Delta G^{\ddagger}$ values for TpRu($PMe_3$)($\eta^2$-$C_2H_4$)-Ph suggest that the rates of ethylene insertion (calculated $\Delta G^{\ddagger}$ of 23.9 kcal/mol) and ethylene C−H activation (calculated $\Delta G^{\ddagger}$ of 27.0 kcal/mol; $\Delta\Delta G^{\ddagger}$ = 3.1 kcal/mol) are likely to be more similar than for the CO system. The relative impact of CO/$PMe_3$ replacement on activation barriers to C−H activation from TpRu(L)(benzene)Ph or TpRu(L)($\eta^2$-$C_2H_4$)Ph is minor with calculated $\Delta\Delta G^{\ddagger}$'s of 1.6 and 0.6 kcal/mol, respectively (see Schemes 7 and 8); however, the impact on ethylene insertion is calculated to be more substantial (Table 5). And, while the $PMe_3$ complex TpRu($PMe_3$)(NCMe)Ph (**2**) might be a more active catalyst for the hydrophenylation of ethylene, we propose that competitive C−H activation of ethylene (in competition with ethylene insertion) results in relatively rapid removal of the active catalyst via formation of the ally complex **5** (Scheme 10).

In addition to the decreased rate of ethylene insertion and, hence, increased predilection toward ethylene C−H activation for the TpRu($PMe_3$) system, the DFT calculations reveal an important steric influence on activation barriers for C−H activation. For C−H activation of benzene by TpRu(L)-(benzene)Ph (L = CO, $PMe_3$, or C≡NH), the DFT calculations suggest that the steric profile of ligand "L" is not inconsequential relative to electronic influence. Thus, although the more electron-rich isonitrile system is calculated to have a lower activation barrier than the CO system, the $PMe_3$ system, which is a more sterically encumbered system, is calculated to have an activation barrier that is greater than the CO complex. For the calculated energetics for benzene C−H activation by TpRu-(L)(benzene)($CH_2CH_2Ph$) (L = CO or $PMe_3$), the $sp^3$ nature of the alkyl ligand (relative to planar $sp^2$ for phenyl) potentially exacerbates the steric influence of "L." Hence, the calculated $\Delta\Delta G^{\ddagger}$ for benzene C−H activation by TpRu(L)(benzene)Ph (L = CO or $PMe_3$) is 1.6 kcal/mol, but the $\Delta\Delta G^{\ddagger}$ for benzene C−H activation by TpRu(L)(benzene)($CH_2CH_2Ph$) (L = CO or $PMe_3$) is more substantial at 6.5 kcal/mol.

## Conclusions

It has been previously predicted from computational studies that an inverse impact on rates of C−H activation and olefin insertion upon increasing metal electron density for TpRu(L)R systems likely places an upper limit on catalyst activity.[39] The reported results are consistent with this notion with the impact of substitution of "L" having a substantial impact on the rate of olefin insertion. Therefore, in the absence of substantial changes in the ligand framework or metal identity/oxidation state, the most important considerations for increasing catalyst efficacy are maintaining a relatively rapid rate of olefin insertion, while controlling regioselectivity, with little impact on the activation barriers to C−H activation relative to TpRu(CO)R systems. Increasing catalyst longevity may also be achieved by moving toward systems that do not possess the CO coligand, which can promote catalyst decomposition via the formation of CO-bridged multinuclear complexes. Such catalysts would incorporate ligands with overall donor ability similar to CO [e.g., $PF_3$ or P(*N*-pyrrolyl)$_3$] or combine an overall cationic metal system with more strongly donating ancillary ligands.

## Experimental Section

**General Methods.** Unless otherwise noted, all synthetic procedures were performed under anaerobic conditions in a nitrogen-filled glovebox or by using standard Schlenk techniques. Glovebox purity was maintained by periodic nitrogen purges and was monitored by an oxygen analyzer [$O_2$(g) < 15 ppm for all reactions]. Benzene, tetrahydrofuran, and diethyl ether (stored over 4 Å molecular sieves) were dried by distillation from sodium/benzophenone. Pentane was distilled over sodium. Acetonitrile and methanol were dried by distillation from $CaH_2$. Hexanes, toluene (stored over 4 Å molecular sieves), and methylene chloride were purified by passage through a column of activated alumina. Acetone-$d_6$, benzene-$d_6$, acetonitrile-$d_3$, and chloroform-$d_1$ were degassed with three freeze−pump−thaw cycles and stored under an $N_2$ atmosphere over 4 Å molecular sieves. $^1$H NMR spectra were recorded on a Varian Mercury 300 or 400 MHz spectrometer, and $^{13}$C NMR (operating frequency 75 MHz) spectra, on a Varian Mercury 300 MHz spectrometer. All $^1$H and $^{13}$C NMR spectra were referenced against residual proton signals ($^1$H NMR) or the $^{13}$C resonances of the deuterated solvent ($^{13}$C NMR). $^{19}$F NMR spectra were obtained on a Varian 300 MHz spectrometer (operating frequency 282 MHz) and referenced against an external standard of hexafluorobenzene ($\delta = -164.9$). $^{31}$P NMR spectra were obtained on a Varian 400 MHz spectrometer and referenced against an external standard of $H_3PO_4$ ($\delta = 0$). $^2$H NMR spectra were obtained on a Varian 500 MHz spectrometer (operating frequency 77 MHz). Resonances due to the Tp ligand in $^1$H NMR spectra are listed by chemical shift and multiplicity only (all coupling constants for the Tp ligand are ∼2 Hz). IR spectra were acquired using a Mattson Genesis II FT-IR as thin films on a NaCl plate. Gas chromatography was performed on a Hewlett-Packard 5890 GC using a J&W DB-1701 capillary column (30 m × 0.25 mm with 0.25 $\mu$m film thickness) and a FID detector. GC-MS was performed using a HP GCD EI system with a 30 m × 0.25 mm HP-5 column with 0.25 mm film thickness. Electron ionizing (EI) mass spectrometry was carried out using a JEOL (Tokyo, Japan) HX110HF high-resolution mass spectrometer at the North Carolina State University Mass Spectrometry Laboratory using perfluorokerosene ions as a reference standard. Ethylene (99.5%) was received in a gas cylinder from MWSC High-Purity Gases and used as received. All other reagents were used as purchased from commercial sources. The preparation, isolation, and characterization of TpRu(CO)(NCMe)Me,[44] TpRu(CO)(NCMe)Ph (**1**),[44] TpRu(PMe$_3$)(NCMe)Ph (**2**),[60] TpRu(CO)(NCMe)(CH$_2$CH$_2$Ph),[45] TpRu(PMe$_3$)(PPh$_3$)Cl,[67] and Mg(vinyl)$_2$[diglyme]$_{1.5}$[68] have been previously reported. Elemental analyses were performed by Atlantic Microlabs, Inc.

**TpRu(PMe$_3$)(NCMe)OTf.** Complex **2** (0.260 g, 0.511 mmol) was added to benzene (35 mL) followed by the addition of triflic acid (47.6 $\mu$L, 0.54 mmol) and stirred for 1 h at room temperature. Any excess triflic acid was quenched with triethylamine. Volatiles were removed in vacuo, the dried solid was dissolved in minimal toluene, and a light yellow solid was precipitated upon addition of approximately 40 mL of hexanes. The precipitate was collected on a fine-porosity frit and dried in vacuo (0.289 g, 0.497 mmol, 97%). $^1$H NMR (acetone-$d_6$, $\delta$): 7.97, 7.95, 7.88, 7.85, 7.67, 7.63 (each 1H, each a d, Tp 3 or 5 position), 6.35 (1H, dt, Tp 4 position), 6.32, 6.24 (each 1H, each a t, Tp 4 position), 2.68 (3H, s, NCC$H_3$), 1.48 (9H, d, $^2J_{HP} = 9$ Hz, P(C$H_3$)$_3$). $^{13}$C{$^1$H} NMR ($C_6D_6$, $\delta$): 145.4, 144.2, 144.0 (d, $J_{CP} = 2$ Hz, Tp 3 and 5 positions), 136.9, 136.3, 134.8 (Tp 3 and 5 positions), 124.5 (N*C*CH$_3$), 119.9 (q, $^1J_{CF} = 319$ Hz, Ru−O$_3$S*C*F$_3$), 106.8, 106.7 (3C total, 1:2 ratio, Tp 4 positions), 15.3 (d, $^1J_{CP} = 27$ Hz, P(*C*H$_3$)$_3$), 3.1 (NC*C*H$_3$). $^{31}$P{$^1$H} NMR ($C_6D_6$, $\delta$): 19.4 (*P*(CH$_3$)$_3$).$^{19}$F{$^1$H} NMR (acetone-$d_6$, $\delta$): −76.9 (C*F*$_3$). HRMS (EI): calcd for $C_{15}H_{22}BF_3N_7O_3$PRuS, 581.0331; found, 581.0323.

**TpRu(PMe$_3$)(NCMe)Me (3).** TpRu(PMe$_3$)(NCMe)OTf (0.289 g, 0.497 mmol) was added to benzene (40 mL) to form a heterogeneous yellow mixture. After addition of Me$_2$Mg[THF]$_2$ (0.099 g, 0.50 mmol), the reaction was stirred for 1 h at room temperature. The yellow heterogeneous mixture was filtered through Celite on a fine-porosity frit. The yellow filtrate was reduced under vacuum, and a solid was precipitated upon addition of hexanes. The light yellow solid was collected over a medium-porosity frit and dried in vacuo (0.148 g, 0.332 mmol, 67%). $^1$H NMR ($C_6D_6$, $\delta$): 7.89, 7.71 (each 1H, each a d, Tp 3 or 5 position), 7.63 (1H, dd, Tp 3 or 5 position), 7.6 (2H, m, overlapping Tp 3 or 5 position), 7.55 (1H, dd, Tp 3 or 5 positions), 6.15 (2H, m, overlapping Tp 4 positions), 5.95 (1H, t, Tp 4 position), 1.21 (9H, d, $^2J_{HP} = 8$ Hz, P(C$H_3$)$_3$), 0.87 (3H, s, NCC$H_3$), 0.64 (3H, d, $^3J_{HP} = 5$ Hz, Ru−C$H_3$). $^{13}$C{$^1$H} NMR ($C_6D_6$, $\delta$): 143.4, 141.9, 140.2, 135.4, 134.8, 134.3 (Tp 3 and 5 positions), 118.4 (N*C*CH$_3$), 105.6 (d, $J_{CP} = 2$ Hz, Tp 4 position), 105.5, 105.2 (Tp 4 positions), 17.1 (d, $^1J_{CP} = 24$ Hz, P(*C*H$_3$)$_3$), 3.4 (NC*C*H$_3$), −6.5 (d, $^2J_{CP} = 12$ Hz, Ru-*C*H$_3$). $^{31}$P{$^1$H} NMR ($C_6D_6$, $\delta$): 21.6 (*P*(CH$_3$)$_3$). CV (CH$_3$CN, TBAH, 100 mV/s): $E_{1/2} = 0.10$ V [Ru(III/II)], 1.29 V [Ru(IV/III), quasi-reversible]. Anal. Calcd for $C_{15}H_{25}BN_7$PRu: C, 40.37; H, 5.65; N, 21.97. Found: C, 40.67; H, 5.70; N, 21.71.

**TpRu(PMe$_3$)(C≡N$^t$Bu)Ph (4).** Complex **2** (0.096 g, 0.19 mmol) and *tert*-butyl isocyanide (64 $\mu$L, 0.60 mmol) were added to benzene (15 mL), and the solution was heated to reflux for 2 h with stirring. The volatiles were removed in vacuo, the solid was dissolved in minimal toluene, and a white solid was precipitated upon addition of approximately 40 mL of hexanes. The precipitate was collected on a fine-porosity frit and dried in vacuo (0.077 g, 0.14 mmol, 75%). IR (thin film on NaCl plate): $\nu_{CN} = 2031$ cm$^{-1}$, $\nu_{BH} = 2478$ cm$^{-1}$. $^1$H NMR ($C_6D_6$, $\delta$): 7.59, 7.55, 7.52 (each 1H, each a d, Tp 3 or 5 position), 7.50 (1H, m, Tp 3 or 5 position), 7.47 (1H, d, Tp 3 or 5 position), 7.50 (1H, m, Tp 3 or 5 position), 7.44, 7.42 (each 1H, each a d, phenyl positions), 7.37 (1H, d, Tp 3 or 5 position), 7.10−7.19 (phenyl resonances overlapping with solvent peak), 6.02, 5.99 (each 1H, each a t, Tp 4 positions), 5.93 (1H, dt, Tp 4 position), 1.10 (9H, d, $^2J_{HP} = 8.1$ Hz, P(C$H_3$)$_3$), 1.09 (9H, s, CNC(C$H_3$)$_3$). $^{13}$C{$^1$H} NMR ($C_6D_6$, $\delta$): 172.1 (d, $^2J_{CP} = 13$ Hz, ipso carbon of phenyl), 144.0, 144.0, 143.9, 143.1, 135.2, 135.0, 134.3 (Tp 3 and 5 positions and phenyl), 125.9, 120.5 (*C*NC(CH$_3$)$_3$ and phenyl), 105.6 (d, $J_{CP} = 2$ Hz, Tp 4 position), 105.7, 105.5 (Tp 4 positions), 56.2 (CN*C*(CH$_3$)$_3$), 32.3 (CNC(*C*H$_3$)$_3$), 18.3 (d, $^1J_{CP} = 26.9$ Hz, P(*C*H$_3$)$_3$). $^{31}$P{$^1$H} NMR ($C_6D_6$, $\delta$): 15.9 (*P*(CH$_3$)$_3$). Anal. Calcd for $H_{33}BC_{22}N_7$PRu: C, 50.19; H, 6.04; N, 17.81. Found: C, 50.31; H, 6.20; N, 17.79.

**TpRu(PMe$_3$)($\eta^3$-C$_4$H$_7$) (5).** Complex **2** (0.096 g, 0.19 mmol) was dissolved in THF (10 mL), and the solution was sealed in a 15 mL pressure reactor, purged with $C_2H_4$, pressurized to 250 psi with $C_2H_4$, and heated to 70 °C for 24 h. The reaction mixture was filtered, and the filtrate was dried in vacuo (0.077 g, 0.17 mmol, 92%). $^1$H NMR ($C_6D_6$, $\delta$): 7.73, 7.66, 7.55, 7.49, 7.45, 6.82 (each 1H, each a d, Tp 3 or 5 position), 6.06, 5.96, 5.77 (each 1H, each t, Tp 4 position), 3.75 (1H, dddd, $^3J_{cb} = 9.6$ Hz, $^3J_{cd} = 9.6$ Hz, $^3J_{cP} = 6.2$ Hz, $^3J_{ca} = 6.3$ Hz, "c"), 2.26 (1H, dd, $^2J_{ab} = 2.6$ Hz, $^3J_{ac} = 6.3$ Hz, "a"), 2.03 (1H, dq, $^3J_{dc} = 9.6$ Hz, $^3J_{dMe} = 6.0$ Hz, "d"), 1.66 (3H, d, $^3J_{dMe} = 6.0$, Me), 1.07 (1H, dd, $^2J_{ba} = 2.1$ Hz,$^3J_{bc} = 9.6$ Hz, "b"), 0.64 (9H, d, $^2J_{HP} = 8$ Hz, P(C$H_3$)$_3$). $^{13}$C NMR ($C_6D_6$, $\delta$): 146.7, 144.2, 140.7, 135.5, 135.2 (Tp 3 and 5 positions), 106.0, 105.5, 105.3 (Tp 4 positions), 85.1 (d, $^1J_{CH} = 150$ Hz, allyl), 50.6 (d, $^1J_{CH} = 150$ Hz, allyl), 30.5 (t, $^1J_{CH} = 152$ Hz, allyl), 19.8 (q, $^1J_{CH} = 123$ Hz, allyl methyl), 15.9 (dq, $^1J_{CH} = 127$ Hz, $^1J_{CP} = 26$ Hz, P(C$H_3$)$_3$). $^{31}$P{$^1$H} NMR ($C_6D_6$, $\delta$): 27.6 (*P*(CH$_3$)$_3$). $^{31}$P heteronuclear multiple bond correlation (HMBC) NMR ($C_6D_6$): P couples with $H_a$, $H_b$, and $H_c$. $^{31}$P selective decoupling at $^1$H $\delta = 0.61$ ppm ($C_6D_6$): 27.6 (d, $^3J_{cP} = 6.2$ Hz, *P*(CH$_3$)$_3$). Anal. Calcd for $C_{16}H_{26}BN_6$PRu: C, 43.16; H, 5.89; N, 18.87. Found: C, 43.74; H, 5.96; N, 18.69.

**TpRu(PMe$_3$)($\eta^2$-C$_2$H$_4$)Ph (6).** TpRu(PMe$_3$)$_2$Ph (0.190 g, 0.350 mmol) was added to benzene (∼40 mL) in a Schlenk flask with a tightly

(67) Slugovc, C. S.; Valentin, N.; Wiede, P.; Mereiter, K.; Schmid, R.; Kirchner, K. *J. Chem. Soc., Dalton Trans.* **1997**, *22*, 4209−4216.
(68) Kobetz, P. Preparation of Divinylic Magnesium Compounds. U.S. Patent 3394197, July 23, 1968.

secured rubber septum, degassed, and backfilled with ethylene. While being stirred, the mixture was irradiated using a 450 W power supply (model no. l7830, Ace Glass, Inc.) equipped with a water-cooled 450 W 5 in. arc IMMER UV−vis lamp (model no. 7825−34, Ace Glass, Inc.) for a total of 24 h until 75% of starting material had converted to **6**. Solvent was reduced, hexanes were added, and a white precipitate was collected on a fine-porosity frit and dried in vacuo (0.060 g, 0.12 mmol, 35%). In various solvents, complex **6** slowly decomposes releasing free ethylene and forming unidentified product(s) preventing full characterization (e.g., clean elemental analysis is not feasible). $^1$H NMR ($C_6D_6$, $\delta$): 7.53, 7.51, 7.43, 7.40, 7.13 (each 1H, each a d, Tp 3 or 5 position), 7.06 (d, Tp 3 or 5 position, partial overlap with phenyl resonances), 7.16 (phenyl resonances overlapping with solvent peak), 6.95 (3H, m, phenyl positions), 6.00, 5.86 (each 1H, each a t, Tp 4 positions), 5.82 (1H, dt, Tp 4 position), 3.24, 2.94 (each 2H, each a m, $\eta^2$-$C_2H_4$) 0.70 (9H, d, $^2J_{HP}$ = 8.1 Hz, P(C$H_3$)$_3$). $^{13}$C{$^1$H} NMR ($C_6D_6$, $\delta$): 170.7 (d, $J_{CP}$ = 13 Hz, phenyl ipso carbon), 145.6, 144.2 (phenyl positions), 143.9, 140.7 (d, $J_{CP}$ = 2 Hz, Tp 3 and 5 position), 135.4, 135.3, 134.7 (Tp 3 and 5 positions), 125.7, 121.1 (phenyl positions), 106.0 (d, $J_{CP}$ = 2 Hz, Tp 4 position), 105.8 (2C, d, $J_{CP}$ = 2 Hz, Tp 4 position), 62.1 (2C; proton-coupled $^{13}$C NMR: t with $^1J_{CH}$ = 158 Hz, $\eta^2$-$C_2H_4$), 15.7 (d, $^1J_{CP}$ = 26.7 Hz, P(C$H_3$)$_3$). $^{31}$P{$^1$H} NMR ($C_6D_6$, $\delta$): 12.9 ($P$(CH$_3$)$_3$).

**TpRu(PMe$_3$)(NCMe)($\eta^1$-C$_2$H$_3$) (9).** TpRu(PMe$_3$)(NCMe)OTf (0.203 g, 0.349 mmol) was added to benzene (35 mL) to form a heterogeneous yellow mixture. After addition of Mg(vinyl)$_2$[diglyme]$_{1.5}$ (0.103 g, 0.368 mmol), the reaction was stirred for 2 h at room temperature. The orange heterogeneous mixture was reduced, pentane was added, and the precipitate was removed via filtration over Celite on a fine-porosity frit. The orange filtrate was reduced, more pentane was added, and the mixture was filtered. The orange filtrate was dried in vacuo to give an orange solid (0.106 g, 0.231 mmol, 66%). $^1$H NMR ($C_6D_6$, $\delta$): 8.83 (1H, ddd, $^3J_{HP}$ = 3.0 Hz, $^3J_{HH}$ = 18.2 Hz, $^3J_{HH}$ = 11.0 Hz, Ru α-vinyl CH), 8.09, 7.70, 7.63, 7.61 (each 1H, each a d, Tp 3 or 5 position), 7.58 (1H, m, Tp 3 or 5 position), 7.56 (1H, d, Tp 3 or 5 position), 6.62 (1H, ddd, $^3J_{HP}$ = 1.7 Hz, $^3J_{HH}$ = 4.6 Hz, $^3J_{HH}$ = 11.0 Hz, Ru $\beta$-vinyl CH), 6.16 (1H, t, Tp 4 positions), 6.09 (1H, dt, Tp 4 positions), 5.96 (1H, t, Tp 4 position), 5.68 (1H, ddd, $^3J_{HP}$ = 1.1 Hz, $^3J_{HH}$ = 4.6 Hz, $^3J_{HH}$ = 18.2 Hz, Ru $\beta$-vinyl CH), 1.18 (9H, d, $^2J_{HP}$ = 8.4 Hz, P(C$H_3$)$_3$), 0.86 (3H, s, NCC$H_3$). $^{13}$C NMR ($C_6D_6$, $\delta$): 177.1 (dddd, $^1J_{CH}$ = 125.3 Hz, $^2J_{CP}$ = 15.6 Hz, $^2J_{CH}$ = 5.0 Hz, $^2J_{CH}$ < 1 Hz (unresolved d), α-C of vinyl), 143.8, 142.2, 141.3 (dt, $^1J_{CH}$ = 181.7−187.5 Hz, $^3J_{CH}$ = $^2J_{CH}$ = 6.9 Hz, Tp 3 or 5 positions), 135.7, 135.0, 134.2 (dt, $^1J_{CH}$ = 184.7−185.8 Hz, triplets unresolved, Tp 3 or 5 positions), 118.9 (q, $^2J_{CH}$ = 9.5 Hz, N$CC$H$_3$), 118.0 (dt, $^1J_{CH}$ = 147.2 Hz, $^3J_{CP}$ ≈ 2 Hz, $\beta$-C of vinyl), 105.6 (dt, $^1J_{CH}$ = 175.2 Hz, $^2J_{CH}$ = 9.1 Hz, Tp 4 position), 105.3 (dt's, overlapping Tp 4 positions), 17.2 [dq (fine splitting also present), $^1J_{CH}$ = 127.0 Hz, $^1J_{CP}$ = 25.2 Hz, P(C$H_3$)$_3$], 3.1 (q, $^1J_{CH}$ = 135.9 Hz, NC$CH_3$). $^{31}$P{$^1$H} NMR ($C_6D_6$, $\delta$): 19.2 ($P$(CH$_3$)$_3$). HRMS (EI): calcd for $C_{16}H_{25}BN_7PRu$, 459.1045; found, 459.1056.

**TpRu(PMe$_3$)(NCMe)Cl (10).** TpRu(PMe$_3$)(PPh$_3$)Cl (0.493 g, 0.717 mmol) was added to acetonitrile (∼40 mL) in a thick-walled pressure tube with a Teflon stopper to give a light-yellow heterogeneous solution. While being stirred, the mixture was irradiated using a 450 W power supply (model no. l7830, Ace Glass, Inc.) equipped with a water-cooled 450 W 5 in. arc IMMER UV−vis lamp (model no. 7825−34, Ace Glass, Inc.) for a total of 24 h. The solution was concentrated to 5 mL under reduced pressure to produce a yellow precipitate. Hexanes (40 mL) were added to the slurry to produce additional precipitate. The precipitate was collected on a fine-porosity frit and dried in vacuo (0.306 g, 0.656 mmol, 92%). $^1$H NMR ($CDCl_3$, $\delta$): 8.02, (1H, s, Tp 3 or 5 position), 7.70 (total 2H, overlapping Tp 3 or 5 position), 7.66 (total 2H, overlapping Tp 3 or 5 position), 7.33 (1H, s, Tp 3 or 5 positions), 6.23 (1H, m, Tp 4 positions), 6.14 (total 2H, overlapping Tp 4 positions), 2.41 (3H, s, NCC$H_3$), 1.44 (9H, d, $^2J_{HP}$ = 7.5 Hz, P(C$H_3$)$_3$). $^{13}$C{$^1$H} NMR (acetone-$d_6$, $\delta$): 145.4, 145.3 (Tp 3 and 5 positions), 142.5 (d, $J_{CP}$ = 2 Hz, Tp 3 or 5 positions), 136.4, 136.0, 134.7 (Tp 3 and 5 positions), 123.1 (N$CCH_3$), 106.5, 105.9 (Tp 4 positions),105.8 (d, $J_{CP}$ = 3 Hz, Tp 4 position), 15.7 (d, $^1J_{CP}$ = 27.3 Hz, P($CH_3$)$_3$), 3.8 (NC$CH_3$). $^{31}$P{$^1$H} NMR ($CDCl_3$, $\delta$): 28.3 ($P$(CH$_3$)$_3$). Anal. Calcd for $RuClPN_7C_{14}BH_{22}$: C, 36.03; H, 4.75; N, 21.01. Found: C, 36.65; H, 4.85; N, 20.80. HRMS (FAB): calcd for $C_{14}H_{13}BClN_7PRu$, 467.0499; found, 467.0494.

**TpRu(CO)($\eta^3$-C$_4$H$_7$) (11).** TpRu(CO)(NCMe)Me (0.113 g, 0.284 mmol) was dissolved in THF (5 mL), and the solution was sealed in a 15 mL pressure reactor, briefly purged with $C_2H_4$, pressurized to 250 psi with $C_2H_4$, and heated to 70 °C for 20 h. The volatiles were removed, and the residue was dried for 2 days in vacuo (0.111 g, 0.279 mmol, 98%). IR (thin film on NaCl plate): $\nu_{CO}$ = 1938 cm$^{-1}$, $\nu_{BH}$ = 2478 cm$^{-1}$. $^1$H NMR ($C_6D_6$, $\delta$): 7.62, 7.57, 7.50, 7.46, 7.32, 6.55 (each 1H, each a d, Tp 3 or 5 position), 5.93, 5.88, 5.66 (each 1H, each a t, Tp 4 position), 4.42 (1H, ddd, $^3J_{CB}$ = 10.9 Hz, $^3J_{CD}$ = 10.8 Hz, $^3J_{CA}$ = 7.0 Hz, "C"), 2.90 (1H, dd, $^3J_{AC}$ = 7.0 Hz, $^2J_{AB}$ = 2.8 Hz, "A"), 2.28 (1H, dq, $^3J_{DC}$ = 10.8 Hz, $^3J_{DMe}$ = 6.0 Hz, "D"), 1.62 (3H, d, $^3J_{MeD}$ = 6.0 Hz, Me), 1.45 (1H, dd, $^3J_{BA}$ = 2.8 Hz, $^3J_{BC}$ = 10.9 Hz, "B"). $^{13}$C-{$^1$H} NMR ($C_6D_6$, $\delta$): 207.8 (*C*O), 146.6, 143.6, 139.1, 135.6, 135.3, 135.2 (Tp 3 and 5 positions), 106.5, 106.4, 105.6 (Tp 4 positions), 92.6, 56.8, 38.7 (allyl), 20.5 (allyl methyl). Anal. Calcd for $C_{14}H_{17}BN_6ORu$: C, 42.33; H, 4.31; N, 21.16. Found: C, 42.54; H, 4.35; N, 20.95.

**Isolation of TpRu(PMe$_3$)(NCMe)Ph-$d_5$ (2-$d_5$).** Complex **2** (∼0.080 g) was dissolved in $C_6D_6$, and the solution was heated in a sealed pressure tube at 60 °C in a temperature-controlled oil bath for 33 h. The reaction mixture was reduced to approximately 0.5 mL of $C_6D_6$, precipitation was induced with the addition of 10 mL of MeOH, and the resultant solid was collected over a frit and dried in vacuo. $^1$H NMR spectroscopy revealed the initial spectrum as previously reported for **2** except that the resonances due to the phenyl ligand were absent. $^2$H NMR spectroscopy revealed broad singlet resonances for the phenyl ligand and Tp-4 positions. $^2$H NMR ($C_6H_6$, $\delta$): 7.25 and 7.10 (phenyl), 5.80 and 5.95 (Tp 4 positions).

**Reaction of TpRu(PMe$_3$)(NCMe)($\eta^1$-C$_2$H$_3$) (9) with HCl.** TpRu-(PMe$_3$)(NCMe)($\eta^1$-C$_2$H$_3$) (**9**) (0.009 g, 0.02 mmol) in $C_6D_6$ under Ar was sealed in a screw-cap NMR tube. HCl (1.0 M in $Et_2O$, 0.019 mL, 0.019 mmol) was added, via microsyringe, and the immediate formation of yellow precipitate was observed. $^1$H NMR analysis revealed the presence of $C_2H_4$ (s, 5.25 ppm). Removal of solvent and reconstitution in $CDCl_3$ showed the complete conversion to TpRu(PMe$_3$)(NCMe)Cl.

**Reaction of TpRu(PMe$_3$)(NCMe)($\eta^1$-C$_2$H$_3$) (9) with C$_6$D$_6$.** To a screw-cap NMR tube was added TpRu(PMe$_3$)(NCMe)($\eta^1$-C$_2$H$_3$) (**9**) (0.007 g, 0.01 mmol) in $C_6D_6$ (0.4 mL) and the sample heated at 70 °C. After 10 h, $^1$H NMR spectroscopy revealed the complete conversion to TpRu(PMe$_3$)(NCMe)Ph-$d_5$ (**2**-$d_5$) and the presence of $C_2H_3D$ (multiplet at 5.25 ppm) and a small amount of $C_2H_4$ (s, 5.25 ppm).

**Reaction of TpRu(PMe$_3$)(NCMe)($\eta^1$-C$_2$H$_3$) (9) with Ethylene.** These reactions were performed in high-pressure J-Young NMR tubes protected by a blast shield. To a high-pressure J-Young tube was added TpRu(PMe$_3$)(NCMe)($\eta^1$-C$_2$H$_3$) (**9**) (0.007, 0.01 mmol) in $C_6D_6$ (0.4 mL). The solution was pressurized to 80 psi with ethylene and heated at 70 °C. Reaction progress was monitored periodically by $^1$H NMR spectroscopy. After 28 h, complete conversion to TpRu(PMe$_3$)($\eta^3$-C$_4$H$_7$) (**5**) was observed by $^1$H NMR spectroscopy.

**Reaction of TpRu(PMe$_3$)(C≡N$^t$Bu)Ph (4) with C$_6$D$_6$.** TpRu-(PMe$_3$)(C≡N$^t$Bu)Ph (**4**) (0.003 mg, 0.006 mmol) was dissolved in $C_6D_6$, sealed in a screw-cap NMR tube and heated at 60 °C. No changes were observed by $^1$H NMR spectroscopy after 3 days.

**Catalytic Hydroarylation Reactions**. A representative catalytic reaction is described. TpRu(PMe$_3$)(NCMe)Ph (**2**) (0.012 g, 0.024 mmol) was dissolved in benzene (2.16 mL), and decane (0.014 mL, 0.072 mmol) was added as an internal standard. The homogeneous reaction mixture was placed in a pressure reactor, charged with 250 psi ethylene

pressure and heated to 60 °C. After 18 h an aliquot of the reaction mixture (~1 μL) was analyzed by GC-FID.

**Catalytic Hydrovinylation Reactions**. A representative catalytic reaction is described. TpRu($PMe_3$)($\eta^3$-$C_4H_7$) (**5**) (0.020 g, 0.045 mmol) was dissolved in THF (4 mL), and the solution was sealed in a 15 mL pressure reactor, briefly purged with $C_2H_4$, pressurized to 300 psi with $C_2H_4$, and heated to 150 °C for 21 h. After depressurization and under nitrogen, an aliquot was withdrawn from the reactor, methylcyclohexane was added as standard, and the sample was analyzed by GC/MS.

**Kinetic Studies: Conversion of TpRu($PMe_3$)(NCMe)Ph (2) or TpRu($PMe_3$)(NCMe)($\eta^1$-$C_2H_3$) (9) and Ethylene to TpRu($PMe_3$)-($\eta^3$-$C_4H_7$) (5).** These reactions were performed in high-pressure J-Young NMR tubes protected by a blast shield. In separate NMR tubes and experiments, TpRu($PMe_3$)(NCMe)Ph (**2**) (0.019 g, 0.037 mmol) and TpRu($PMe_3$)(NCMe)($\eta^1$-$C_2H_3$) (**9**) (0.018, 0.039 mmol), each with a small crystal of hexamethylbenzene (as internal standard), were dissolved in THF-$d_8$ (0.60 mL and 0.63 mL, respectively), and the solutions were placed in J-Young NMR tubes, pressurized to 80 psi with $C_2H_4$, and heated to 60 °C. Periodically, the reactions were analyzed by $^1$H NMR spectroscopy, and concentrations of starting material, intermediates, and products were determined. Reactions were monitored through at least 90% conversion. Rate constants given in the Results are an average of two experiments and kinetic simulation using KINSIM/FITSIM software (errors are a result of simulated fits to kinetic plots; see Supporting Information).

**Kinetic Studies: Conversion of TpRu(CO)(NCMe)Ph (1) and Ethylene to TpRu(CO)($\eta^3$-$C_4H_7$) (11).** These reactions were performed in high-pressure J-Young NMR tubes protected by a blast shield. TpRu-(CO)(NCMe)Ph (**1**) (0.017 g, 0.037 mmol) and a small crystal of hexamethylbenzene (as internal standard) was dissolved in THF-$d_8$ (0.60 mL), and the solutions were placed in a J-Young NMR tube, pressurized to 80 psi with $C_2H_4$, and heated to 60 °C. Periodically, the reactions were analyzed by $^1$H NMR spectroscopy, and concentrations of starting material, intermediates, and products were determined. Reactions were monitored through at least 90% conversion. Multiple experimental runs revealed reproducible results. The production of ethylbenzene was confirmed by GC-MS.

**Observation of TpRu($PMe_3$)($C_2H_4$)($\eta^1$-$C_2H_3$) (7).** These reactions were performed in high-pressure J-Young NMR tubes protected by a blast shield. Complex **7** has not been isolated. Evidence for the presence of **7** during the formation of allyl complex **5** is derived from $^1$H NMR spectroscopy from the separate reactions of TpRu($PMe_3$)(NCMe)Ph (**2**) and TpRu($PMe_3$)(NCMe)(n$^1$-$C_2H_3$) (**9**) under 80 psi ethylene pressure in THF-$d_8$ (see above). For both reactions, complex **7** is observed as a reaction intermediate by $^1$H NMR. The following NMR data are taken from the reaction of **9** and ethylene to form **5**. $^1$H NMR (THF-$d_8$; $\delta$): 8.19 (1H, ddd, $^3J_{HP}$ = 5.7 Hz, $^3J_{HH}$ = 18.0 Hz, $^3J_{HH}$ = 10.8 Hz, Ru α-vinyl CH), 7.84, 7.54, 7.04 (each 1H,each a d, Tp 3 or 5 position), 5.57 (1H, ddd, $^3J_{HP}$ = 1.8 Hz, $^3J_{HH}$ = 3.3 Hz, $^3J_{HH}$ = 10.8 Hz, Ru $\beta$-vinyl CH), 4.40 (1H, dd, $^3J_{HH}$ = 3.3 Hz, $^3J_{HH}$ = 18.0 Hz, Ru $\beta$-vinyl CH), 2.85, 2.44 (each 2H, each a multiplet, $C_2H_4$), 1.03 (9H, d, $^2J_{HP}$ = 7.8 Hz, P($CH_3$)$_3$). *Note*: The observation of only 3 of 9 Tp resonances is due to coincident overlap with other complexes.

**KIE Determination for Benzene Activation by TpRu($PMe_3$)-(NCMe)Me (3).** Individual samples of **3** (0.030 g, 0.067 mmol) in a 1:1 molar mixture of $C_6D_6$/$C_6H_6$ (359 μL:360 μL) were prepared, placed in J-Young tubes, and heated (70 °C) for approximately 4.5 h (~3 half-lives). After 1 and 3 half-lives the samples were cooled to room temperature in a water bath and shaken, and $^1$H NMR spectra (400 MHz) were acquired (pulse delay of 5 s) to measure the ratio of $CH_4$ ($\delta$ = 0.16 ppm, s) to $CH_3D$ ($\delta$ = 0.15 ppm, 1:1:1 t, $^1J_{HD}$ = 2 Hz).

**Kinetic Studies: Rate of Acetonitrile Dissociation for TpRu-($PMe_3$)(NCMe)Ph (2).** A solution of **2** (0.016 g, 0.031 mmol) in 2.5 mL of $CD_3CN$, with a small crystal of hexamethylbenzene as standard, was divided among 3 screw-cap NMR tubes. The triplicate set was heated at 60 °C in a temperature-regulated oil bath, $^1$H NMR spectra were periodically acquired through 3 half-lives (using a pulse delay of 10 s). Acetonitrile dissociation was followed by integration of the decreasing resonance due to coordinated $NCCH_3$ at 2.31 ppm relative to the standard hexamethylbenzene.

**Kinetic Studies: Dependence of H/D Exchange by TpRu($PMe_3$)-(NCMe)Ph (2) in $C_6D_6$ on Concentration of Free Acetonitrile.** A solution of **2** (0.033 g, 0.065 mmol) and either 0, 1 (3.4 μL, 0.07 mmol), 2 (6.8 μL, 0.13 mmol), or 3 (10.3 μL, 0.20 mmol) equiv of dry acetonitrile in 2 mL of $C_6D_6$ with a small crystal of hexamethylbenzene as standard was divided among 3 screw-cap NMR tubes. The set was heated at 60 °C in a temperature-regulated oil bath. $^1$H NMR spectra were periodically acquired through 3 half-lives (using a pulse delay of 10 s). H/D exchange was followed by integration of the decreasing phenyl resonance at 7.45 ppm relative to the standard hexamethylbenzene. The $k_{obs}$ was determined from a linear plot of ln [**2**] versus time (sample kinetic plots are provided in the Supporting Information).

**Kinetic Studies: Temperature Dependence of Catalytic H/D Exchange Rate by TpRu($PMe_3$)(NCMe)Ph in $C_6D_6$.** A solution of **2** (0.033 g, 0.065 mmol) in 2 mL of $C_6D_6$ with a small crystal of hexamethylbenzene (standard) was divided among 4 screw-cap NMR tubes. The mixtures were separately heated at 50, 60, 70, or 80 °C in a temperature-regulated oil bath. $^1$H NMR spectra were periodically acquired through 3 half-lives (using a pulse delay of 10 s). H/D exchange was followed by integration of the decreasing phenyl resonance at 7.45 ppm relative to the standard hexamethylbenzene.

**Computational Methods.** As full experimental ligand models were studied, the MOE program[69] and the MMFF94[70] force field were initially used to identify the lowest energy conformations for subsequent refinement of geometries with DFT methods. All quantum calculations employed the Gaussian03 package.[71] The B3LYP functional (Becke's three-parameter hybrid functional[72] using the LYP correlation functional containing both local and nonlocal terms of Lee, Yang, and Parr)[73] and VWN (Slater local exchange functional[74] plus the local correlation functional of Vosko, Wilk, and Nusair)[75] were employed in conjunction with the Stevens (SBK) valence basis sets and effective core potentials for all heavy atoms and the −31G basis set for hydrogen. The SBK valence basis sets are valence triplet-ζ for ruthenium and double-ζ for main group elements. The basis sets of main group elements are augmented with a d-polarization function: $\xi_d$ = 0.8 for boron, carbon, nitrogen, and oxygen; $\xi_d$ = 0.55 for phosphorus. The SBK scheme utilizes a semicore (46-electron core) approximation for ruthenium and a full core approximation for main group elements. All complexes modeled are closed-shell (diamagnetic) species and were modeled within the restricted Kohn−Sham formalism. All systems were fully optimized without symmetry constraint, and analytic calculations of the energy Hessian were performed to confirm species as minima or transition states and to obtain free energies (using unscaled vibrational frequencies) in the gas phase at 1 atm and 298.15 K.

**Acknowledgment.** T.B.G. acknowledges the Office of Basic Energy Sciences, U.S. Department of Energy (Grant No. DE-FG02-03ER15490), for support of this research. T.R.C. acknowledges the U.S. Department of Education for its support of the CASCaM facility. The research at UNT was supported in part by a grant from the Offices of Basic Energy Sciences, U.S. Department of Energy (Grant Nos. DEFG02-03ER15387). Calculations employed the UNT computational chemistry resource, which is supported by the NSF through Grant CHE-

(69) Chemical Computing Group, version 2005.06. http://www.chemcomp.com/.
(70) Halgren, T. A. *J. Comput. Chem.* **1996**, *17*, 616−641.
(71) Frisch, M. J.; et al. *Gaussian 03*, revision C.02; Gaussian, Inc.: Wallingford, CT, 2004 (see Supporting Information for full reference).
(72) Becke, A. D. *J. Chem. Phys.* **1993**, *98*, 1372−1377.
(73) Lee, C.; Yang, W.; Parr, R. G. *Phys. Rev.* **1998**, *B37*, 785−789.
(74) Kohn, W.; Sham, L. *Phys. Rev.* **1980**, *A140*, 1133.
(75) Vosko, S. H. W. L.; Nusair, M. *Can. J. Chem.* **1980**, *58*, 1200−1211.

0342824. T.R.C. also acknowledges the Chemical Computing Group for generously providing the MOE software. Mass spectra were obtained at the North Carolina State University Mass Spectrometry Laboratory. Partial funding for the Facility was obtained from the North Carolina State University Department of Chemistry, North Carolina Biotechnology Center, and the National Science Foundation. We thank Dr. William Jones (U. of Rochester) for assistance with kinetic simulation and Dr. Sabapathy Sankar (NCSU) for assistance with advanced NMR techniques.

**Supporting Information Available:** Details of kinetic simulations, sample kinetic plots, X-ray structural analyses of complexes **3**, **4**, and **10**, and complete reference 71. This material is available free of charge via the Internet at http://pubs.acs.org.

JA068542P